($^{15}N_5$)-Labeled Adenine Derivatives: Synthesis and Studies of Tautomerism by ^{15}N NMR Spectroscopy and Theoretical Calculations

Avital Laxer, Dan T. Major, Hugo E. Gottlieb, and Bilha Fischer*

Department of Chemistry, Gonda-Goldschmied Medical Research Center, Bar-Ilan University, Ramat-Gan 52900, Israel

bfischer@mail.biu.ac.il

Received April 2, 2001

Since the nitrogens of nucleosides and nucleotides play an important role in the molecular recognition of these compounds, ^{15}N NMR became a method of choice in this field. Fully ^{15}N-labeled adenine, required in the latter studies, was obtained in four synthetic steps, in a good yield. Likewise, ($^{15}N_5$)-2-hexylthioether-adenine and ($^{15}N_5$)-8-Br-adenine were obtained in five synthetic steps from the relatively inexpensive ^{15}N sources: ^{15}N-NH_4Cl, ^{15}N-NH_4OH, ^{15}N-$NaNO_2$. Full ^{15}N labeling of these adenine prototypes enabled to obtain high-resolution ^{15}N NMR spectra of these bases at 60.8 MHz. Furthermore, the spectra suggested the existence of the N3-H species in the tautomeric mixtures of these compounds in solution, in addition to the well-reported N9-H (major) and N7-H (minor) tautomers. These observations were also supported by quantum mechanical calculations of the tautomeric equilibria in the gas phase and in solution of the above-mentioned adenine compounds. The gas-phase tautomeric equilibria were estimated using density functional theory and second-order perturbation theory methods. Solvent effects were included by means of both continuum and discrete solvation models. The observation of the existence of the N3-H tautomer has a clear impact on the possible H-bonding patterns of these adenine prototypes and on their molecular recognition by various biological macromolecules. The above^{15}N-labeled analogues are expected to find use as ^{15}N NMR probes for numerous biochemical studies.

Introduction

^{15}N NMR is a powerful tool for determining structure, function, and molecular recognition phenomena within proteins, nucleic acids, and other nitrogen containing molecules of biological importance.[1] The suitability of ^{15}N NMR spectroscopy for these studies is attributed to the wide range of chemical shifts (900 ppm) and its great sensitivity to structural and environmental changes (e.g., H-bonds, protonation). However, a major disadvantage of this spectroscopy is the extremely low sensitivity of ^{15}N at natural abundance level, which is 3.8×10^{-6} of that of a proton at constant magnetic field.[1] Although natural abundance ^{15}N NMR studies of various molecules and macromolecules have been reported,[2] selective ^{15}N enrichment is needed for obtaining spectra of these molecules within practical time limits. In addition, ^{15}N enrichment of small molecule probes is essential for evaluating their interactions with biological macromolecules, without measuring the multitude nitrogen signals of proteins or nucleic acids.

Since the nitrogens of nucleosides and nucleotides play an important role in the molecular recognition of these compounds, either as monomers or within nucleic acids fragments, ^{15}N NMR became a method of choice in this field as reflected in numerous studies. ^{15}N NMR spectra of several nucleosides and nucleotides have been obtained at natural abundance and for singly labeled and uniformly biosynthetically ^{15}N-enriched adenine.[3]

Most reports describing ^{15}N-labeling of adenine nucleosides refer to a single label at either N1, N3, N^6, N7, or N9.[4−8] Several syntheses of doubly labeled adenine (adenosine) are also known, at N1 and N^6, N^6 and N7, N^6 and N9, or N1 and N7 positions.[9−12]

* To whom correspondence should be addressed. Fax: 972-3-5351250. Tel.: 972-3-5318303.

(1) (a) Kanamori, K.; Roberts, J. D. ^{15}N NMR studies of biological systems. *Acc. Chem. Res.* **1983**, *16*, 35−41. (b) Berger, S.; Braun, S.; Kalinowski, H.-O. *NMR spectroscopy of the nonmetallic elements*; John Wiley: New York, 1996; Chapter 4, pp 229−237.

(2) Gust, D.; Moon, R. B.; Roberts, J. D. Applications of natural-abundance nitrogen- 15 nuclear magnetic resonance to large biochemically important molecules. *Proc. Natl. Acad. Sci. U.S.A.* **1975**, *72*, 4696−4700.

(3) (a) Markowski, V.; Sullivan, G. R.; Roberts, J. D. Nitrogen-15 nuclear magnetic resonance spectroscopy of some nucleosides and nucleotides. *J. Am. Chem. Soc.* **1977**, *99*, 714−718. (b) Gonnella, N. C.; Nakanishi, H.; Holtwick, J. B.; Horowitz, D. S.; Kanamori, K.; Leonard, N. J.; Roberts, J. D. Studies of tautomers and protonation of adenine and its derivatives by nitrogen-15 nuclear magnetic resonance spectroscopy. *J. Am. Chem. Soc.* **1983**, *105*, 2050−2055. (c) Büchner, C.; Maurer, W.; Rüterjans, H. Nitrogen-15 nuclear magnetic resonance spectroscopy of ^{15}N-labeled nucleotides. *J. Magn. Reson.* **1978**, *29*, 45−63.

(4) a. Kos, N. J.; van der Plas, H. C. Occurrence of the S_NANRORC mechanism in the amination of 2-sustituted purines with potassium amide in liquid ammonia. *J. Org. Chem.* **1980**, *45*, 2942−5, b. Gao, X.; Jones, R. A. Nitrogen-15-labeled deoxynucleosides. Synthesis of [6-^{15}N]- and [1-^{15}N]deoxyadenosines from deoxyadenosine. *J. Am. Chem. Soc.* **1987**, *109*, 1275−1278. c. del Carmen M.; Barrio, G.; Scopes, D. I. C.; Holtwick, J. B.; Leonard, N. J. Syntheses of all singly labeled [^{15}N]-adenines: Mass spectral fragmentation of adenine. *Proc. Natl. Acad. Sci. U.S.A.* **1981**, *78*, 3986−3988.

(5) Rhee, Y.-S.; Jones, R. A. Nitrogen-15-labeled deoxynucleosides. 3. Synthesis of [3-^{15}N]-2′- deoxyadenosine. *J. Am. Chem. Soc.* **1990**, *112*, 8174−8175.

(6) (a) Kos, N. J.; van der Plas, H. C.; van Veldhuizen, B. The Chichibabin reaction of purines with potassium amide in liquid ammonia. *J. Org. Chem.* **1980**, *45*, 2942−5. (b) Gao, X.; Jones, R. A. Nitrogen-15-labeled deoxynucleosides. Synthesis of [6-^{15}N]-and [1-^{15}N] deoxyadenosines from deoxyadenosine. *J. Am. Chem. Soc.* **1987**, *109*, 1275−1278.

10.1021/jo010344n CCC: $20.00
Published on Web 07/17/2001

Purines and pyrimidine bases or nucleosides specifically labeled with ^{15}N are used for various applications: (1) investigation of possible H-bonds among nucleosides (base pairing);[13] (2) evaluation of tautomeric equilibria in purine bases;[3b] (3) probing metal complexes with purine ring nitrogens in ATP;[14] (4) monitoring DNA major groove interactions with small molecules[15] and drugs;[16] (5) investigation of DNA/protein complexes, using ^{15}N isotope-edited NMR[17] or HMQC techniques;[18] (6) conformational analysis of nucleotides;[19] (7) incorporation of the labeled nucleosides into nucleic acid fragments and elucidation of their structure; fully or partially ^{15}N- and ^{13}C-labeled RNA fragments[20] have been used to provide 3D structural information[15] applying double and triple resonance NMR methods; (8) probing protonation of nucleotides in monomers or nucleic acid fragments[21] and for determining their pD values.[22]

The latter application is based on the fact that the chemical shift of ^{15}N changes drastically upon protonation and can be clearly monitored by ^{15}N NMR spectroscopy.[23] Furthermore, it is possible to determine if a nitrogen atom is involved in H-binding and the type of H-bond, i.e., acceptor or donor.[1,13]

Environmental changes, e.g., the presence of a protein, affect the ^{15}N chemical shift. Therefore, labeling the base/nucleoside/nucleotide probe at all nitrogen positions is important for isolating local effects, due to specific binding interactions, from environmental effects, which influence the whole molecule. Labeling all nitrogen positions enables the use of a single NMR probe instead of up to five singly labeled probes.

The production of uniformly labeled adenine was acieved from *S*-adenosyl methionine by yeast biosynthesis in a medium containing ^{15}N-ammonium chloride.[24] This preparation resulted in 41% ^{15}N content in the product based on mass spectrometry. ^{15}N-enrichment of 90% was claimed for nucleosides-3′-phosphates. The latter were obtained through the isolation of ribosomes from E. Coli grown on $(^{15}NH_4)_2SO_4$ and preparation of labeled ribosomal RNA, followed by enzymatic degradation and separation.[3c] High ^{15}N enrichment of the probe is most important for practical measurement times of ^{15}N NMR spectra (i.e., for a comparable spectrum, 100% enrichment allows for shortening the measurement time by a factor of 73 000 compared with natural abundance). Furthermore, high enrichment is important for obtaining structural information through $^{15}N-^{15}N$ couplings. Despite the interest in uniformly 100% ^{15}N-enriched adenine bases and nucleotides, their preparation by chemical means has not been reported so far.

In this paper, we wish to report the first synthesis of $(^{15}N_5)$-labeled adenine and related analogues as well as their spectral properties and high-resolution ^{15}N NMR spectra. Tautomeric equilibria of these purine derivatives are discussed based on their ^{15}N NMR spectra and quantum mechanical calculations including solvent effects either by continuum models (polarizable continuum model and finite difference Poisson−Boltzmann model) or explicit solvent molecules model. The new probes are expected to find use in ^{15}N NMR studies of molecular recognition of numerous nucleoside/nucleotide-binding proteins. Likewise, these labeled derivatives can be introduced into nucleic acids fragments for structural and functional studies applying ^{15}N NMR spectroscopy.

Results

Synthesis. In this study, we aimed at the synthesis of three $(^{15}N_5)$-labeled adenine derivatives—the parent adenine compound, **1**, 2-hexylthio-adenine,[25a] **2**, and 8-Br-

(7) Gaffney, B. L.; Kung P.-P.; Jones, R. A. Nitrogen-15-labeled deoxynucleosides. 2. Synthesis of [7-^{15}N]-labeled deoxyadenosine, deoxyguanosine, and related deoxynucleosides. *J. Am. Chem. Soc.* **1990**, *112*, 6748−6749.

(8) Orji, C.; Kelly, J.; Ashburn, D. A.; Silks, L. A., III. First synthesis of b-2′-deoxy[9-^{15}N]adenosine. *J. Chem. Soc., Perkin Trans. 1* **1996**, 595−597.

(9) Ariza, X.; Bou, V.; Vilarrasa, J. A new route to ^{15}N-labeled, N-alkyl, and N-amino nucleosides via N-nitration of uridines and inosines. *J. Am. Chem. Soc.* **1995**, *117*, 3665−3673.

(10) Pagano, A. R.; Lajewski W. M.; Jones, R. A. Syntheses of [6,7-^{15}N]-adenosine, [6, 7-^{15}N]-deoxyadenosine, and [7-^{15}N]-hypoxanthine. *J. Am. Chem. Soc.* **1995**, *117*, 11669−11672.

(11) Orji, C.; Silks, L. A., III. The first synthesis of [9, amino-$^{15}N_2$] adenine and b-2′-deoxy[9, amino-$^{15}N_2$] adenosine. *J. Label. Comp. Radio Pharm.* **1995**, 625−630.

(12) Pagano, A. R.; Zhao, H.; Shallop, A.; Jones, R. A. Syntheses of [1,7-N-^{15}(2)]-and [1,7-N-^{15}(3)]-adenosine and 2′-deoxyadenosine via an N-1-alkoxy-mediated Dimroth rearrangement. *J. Org. Chem.* **1998**, *63*, 3213−3217.

(13) (a) Dunger, A.; Limbach, H. H.; Weisz, K. NMR studies on the self-association of uridine and uridine analogues. *Chem. Eur. J.* **1998**, *4*, 621−628. (b) Gaffney, B. L.; Kung, P. P.; Wang, C.; Jones, R. A. Nitrogen-15-labeled oligodeoxynucleotides 8. Use of N-15 NMR to probe Hoogsteen hydrogen-bonding at guanine and adenine N7 atoms of a DNA triplex. *J. Am. Chem. Soc.* **1995**, *117*, 12281−12283.

(14) (a) Happe, J. A.; Morales, M. Nitrogen-15 nuclear magnetic resonance evidence that Mg^{2+} does not complex with nitrogen atoms of adenosine triphosphate. *J. Am. Chem. Soc.* **1966**, *88*, 2077−2078. (b) Qu, Y.; Farrell, N. Association of mononuclear and dinuclear platinum tetraamine cations with nucleotides studied by N-15 NMR relaxation. *Inorg. Chim. Acta* **1996**, *245*, 265−267.

(15) Gaffney, B. L.; Wang, C.; Roger, R. A. Nitrogen 15-labeled oligodeoxynucleotides. 4. Tetraplex Formation of d[G(^{15}N^7)GTTTTTGG] and d[T(^{15}N^7)GGGT] Monitored by ^{1}H Detected ^{15}N NMR. *J. Am. Chem. Soc.* **1992**, *114*, 4047−4050.

(16) Rhee, Y.; Wang, C.; Gaffney, B. L.; Roger, R. A. Nitrogen 15-labeled oligodeoxynucleotides. 6. Use of ^{15}N NMR to probe binding of Netropsin and Distamycin to {d[CGCGAATTCGCG]}$_2$. *J. Am. Chem. Soc.* **1993**, *115*, 8742−8746.

(17) MacMillan, M. A.; Lee, R. J.; Verdine, G. L. Direct observation of a specific contact in the λ repressor-O_L1 complex by isotope-edited NMR. *J. Am. Chem. Soc.* **1993**, *115*, 4921−4922.

(18) Sklenar, V.; Peterson, R. D.; Rejante, M. R.; Wang, E.; Feigon, J. Two-dimensional triple resonance HCNCH experiment for direct correlation of ribose H1′ and base H8, H6 protons in ^{13}C, ^{15}N-labeled RNA oligonucleotides. *J. Am. Chem. Soc.* **1993**, *115*, 12181−12182.

(19) Ippel, J. H.; Wijmenga, S. S.; deJong, R.; Heus, H. A.; Hilbers, C. W.; deVroom, E.; vanderMarel, G. A.; vanBoom, J. H. Heteronuclear scalar couplings in the bases and sugar rings of nucleic acids: their determination and application in assignment and conformational analysis. *Magn. Reson. Chem.* **1996**, *34*, S156−S157.

(20) (a) Abad, J. L.; Shallop, A. J.; Gaffney, B. L.; Jones, R. A. Use of C-13 tags with specifically N-15-labeled DNA and RNA. *Biopolymers* **1998**, *48*, 57−63. (b) Zhao, H.; Pagano, A. R.; Wang, W. M.; Shallop, A.; Gaffney, B. L.; Jones, R. A. Use of a C-13 atom to differntiate two N-15-labeled nucleosides. Syntheses of [(NH_2)-N-15]-adenosine, [1-NH_2-N-15(2)]-and [[2-C-13-1-NH_2-N-15(2)]guanosine, -and [1,7-NH_2-N-15-(3)]- and [2-C-13-1,7-NH_2-N-15(3)]-2′-deoxyguanosine. *J. Org. Chem.* **1997**, *62*, 7832−7835.

(21) Massefski, W.; Redfield, A.; Das Sarma, U.; Bannerji, A.; Roy, S. [7-^{15}N] Guanosine labeled oligonucleotides as nuclear magnetic resonance probes for protein-nucleic acid interaction in the major groove. *J. Am. Chem. Soc.* **1990**, *112*, 5350−5351.

(22) Buchanan, G. W. Application of ^{15}N NMR spectroscopy to the study of molecular structure, stereochemistry and binding phenomena. *Tetrahedron* **1989**, *45*, 581−604.

(23) Wang, C.; Gao, H.; Gaffney, B. L.; Roger, R. A. Nitrogen 15-labeled oligodeoxynucleotides. 3. Protonation of the adenine N1 in the A·C and A·G mispairs of the duplexes {d[CG(^{15}N^1)AGAATTCCCG]}$_2$ and {d[CGGGAATTC(^{15}N^1)ACG]}$_2$. *J. Am. Chem. Soc.* **1991**, *113*, 5486-5488.

(24) Zappia, V.; Salvatore, F.; Zydek, C. R.; Schlenk, F. The production of ^{15}N-labeled S-adenosylmethionine and adenine by yeast biosynthesis. *J. Labeled Comp.* **1968**, *4*, 230−239.

(25) (a) Kikugawa, K.; Suehiro, H.; Aoki, A. Platelet aggregation inhibitors. VIII. 2-thioadenine derivatives. *Chem. Pharm. Bull.* **1977**, *25*, 1811−1821. (b) Naidis, F. B.; Kolesova, M. B.; Aleksander, K. L.; Smirnova, N. V.; Pernikoza, V. G. Method of obtaining 8-bromoadenine. *Izobreteniya* **1995**, *1*, 242.

adenine,[25b] **3**. These analogues are targeted as prototypes for analyzing the effect of electron donating and electron withdrawing groups on the adenine ring on the tautomeric equilibria and pK_a of this ring system, utilizing ^{15}N NMR spectroscopy. Furthermore, investigation of the effect of 8-Br and 2-thiohexyl substituents on the interaction of adenine nucleosides and nucleotides with various proteins applying ^{15}N NMR experiments is yet another goal. These questions are currently under investigation in our laboratory.

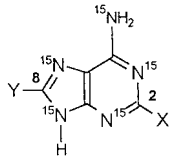

1, X = H, Y = H
2, X = S(CH$_2$)$_5$CH$_3$, Y = H
3, X = H, Y = Br

Two approaches have been employed for the synthesis of singly or doubly ^{15}N-labeled nucleosides:[26a] (1) Transformation of intact nucleosides to singly ^{15}N-labeled nucleosides based on some type of rearrangement of the purine ring system like the Dimroth rearrangement,[4b,26b−d] or related ring-opening−ring-closure reactions triggered by N1-nitration, amination, or methoxylation.[9,27] (2) De novo synthesis, namely, the appropriately ^{15}N-labeled heterocycles are synthesized by building the azole or the azine ring upon the other one, with the incorporation of the label at a suitable step, and condensed with appropriate sugars to furnish the desired nucleosides.

For the introduction of five labeled nitrogens into an adenine, only the second synthetic route is applicable. We planned the assembly of all five labeled nitrogens on a pyrimidine ring, **7**, in only two synthetic steps based on the Traube synthesis[28] leading to pyrimidine, **6**, followed by nitrosation of the latter (Schemes 1 and 2).

Synthetic routes in which expensive isotopically labeled reagents are used should be planned according to the following rules: (a) minimal number of synthetic steps; (b) high yields; (c) as low number of labeled reagent equivalents as possible; and (d) a good method for recovery of unreacted labeled reagents or intermediates.

Gathering four labeled nitrogens on Traube pyrimidine, **6**, requires the preparation of ($^{15}N_2$)-malononitrile [29] and ($^{15}N_2$)-thiourea[30] (Scheme 3).

Recently, we reported the first synthesis of doubly ^{15}N-labeled malononitrile.[29] Highly pure ($^{15}N_2$)-malononitrile

Scheme 1. Retrosynthetic Plan for Preparation of Fully ^{15}N-Labeled Adenine Derivatives

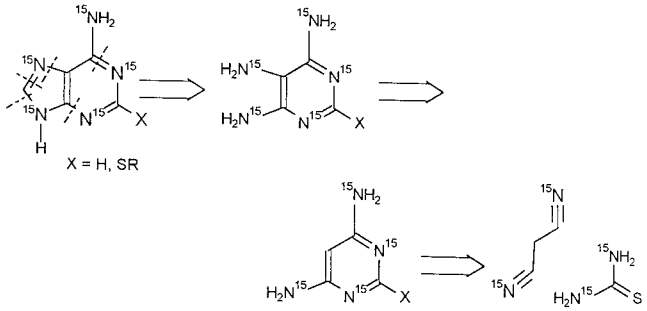

Scheme 2. Assembly of All Five ^{15}N Atoms on Pyrimidine 7 in Two Steps[a]

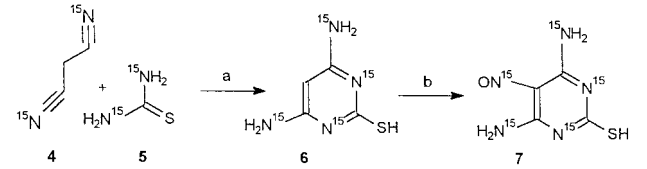

[a] Key: (a) EtONa/EtOH/reflux/3 h, 71%; (b) Na$^{15}NO_2$/HOAc−H_2O/0 °C/3 h, 57%.

Scheme 3. Preparation of Starting Materials[a]

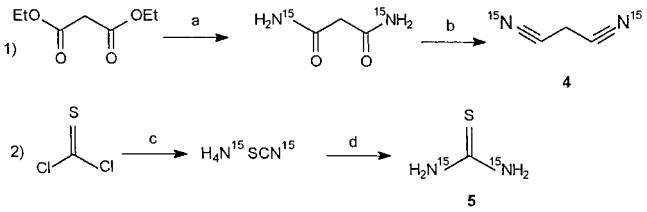

[a] Key: (a) 7 N $^{15}NH_4OH$/rt/overnight, 84%; (b) $POCl_3$/CH_3CN/reflux/4 h, 75%; (c) $^{15}NH_4Cl$/NaOH/silica gel column/Chelex $^{15}NH_4^+$, 85%; (d) 190 °C/2 h/silica gel column, 12%.

was obtained in a facile and simple two-step synthesis that includes reaction of diethyl malonate with 25% $^{15}NH_4OH$ at room temperature overnight to form ($^{15}N_2$)-malonodiamide in 84% yield and dehydration of the latter by $POCl_3$ in acetonitrile to ($^{15}N_2$)-malononitrile in 75% yield, Scheme 3.

The synthesis of $^{15}N_2$-thiourea from ($^{15}N_2$)-ammonium thiocyanate has been reported recently.[30a] ($^{15}N_2$)-Ammonium thiocyanate was prepared in turn from thiophosgene and $^{15}NH_4Cl$ in an aqueous NaOH solution.[30a] A major disadvantage of both these procedures is the very high vacuum, which is not readily accessible, required for purification by sublimation of ($^{15}N_2$)-ammonium thiocyanate and ($^{15}N_2$)-thiourea. Therefore, we modified the original procedure to afford a facile workup resulting in a higher yield (85%) of ($^{15}N_2$)-ammonium thiocyanate after one round of the reaction. The crude mixture obtained from reaction of thiophosgene and $^{15}NH_4Cl$ in an aqueous NaOH solution, was easily separated on a silica gel column. ($^{15}N_2$)-Ammonium thiocyanate was eluted with $CHCl_3$/MeOH and detected on TLC as a yellow spot by dipping in $KMnO_4$ solution. ^{15}N NMR spectrum in water showed two singlets at −175 ppm

(26) (a) Sako, M. Syntheses of N-15-labeled nucleosides. *J. Synth. Org. Chem. Jpn.* **1996**, *54*, 54−61. (b) Fujii, T.; Itaya, T. The Dimroth rearrangement in the adenine series: A review updated. *Heterocycles* **1998**, *48*, 359−390. (c) Wilson, M. H.; McCloskey, J. A. Isotopic labeling studies of the base-catalyzed conversion of 1-methyladenosine to N^6-methyladenosine. *J. Org. Chem.* **1973**, *38*, 2247. (d) Sarfati, S. R.; Kansal, V. K. Synthesis of 6-^{15}N and 1-^{15}N labeled adenosine monophosphates. *Tetrahedron* **1988**, *44*, 6367−6372.

(27) (a) Goswami, B.; Jones, R. A. Nitrogen-15-labeled deoxynucleosides. 4. Synthesis of [1-^{15}N]-and [2-^{15}N]-labeled 2′-deoxyguanosines. *J. Am. Chem. Soc.* **1991**, *113*, 644−647. (b) Kos, N. J.; Jongejan, H.; van der Plas, H. C. Deamination, involving ring opening in reactions of 1-aminopurinium mesitylenesulfonates with methanolic ammonia. *Tetrahedron* **1987**, *43*, 4841−4848. (c) Pagano, A. R.; Zhao, H.; Shallop, A.; Jones, R. A. Syntheses of [1,7-N-15(2)]- and [1,7-NH_2-N-15(3)]-adenosine and 2′-deoxyadenosine via an N-1-alkoxy-mediated Dimroth rearrangement. *J. Org. Chem.* **1998**, *63*, 3213−3217.

(28) (a) Traube, W. *Ann.* **1904**, *331*, 64. (b) Benedich, A.; Tinker, J. F.; Brown, G. B. A synthesis of isoguanosine labeled with isotopic nitrogen. *J. Am. Chem. Soc.* **1948**, *70*, 3109−3113.

(29) Laxer, A.; Fischer, B. A facile synthesis of ($^{15}N_2$) malononitrile. *J. Labeled Comp. Radiopharm.* **2000**, *43*, 47−53.

(30) (a) Amantea, A.; Henz, M.; Strazewski, P. 24. Synthesis of ($^{15}N_2$)[^{17}O]urea, ($^{15}N_2$)[O^2, O^4-^{17}O]uridine, and ($^{15}N_3$)[$O^{2-17}O$]cytidine. *Helv. Chim. Acta* **1996**, *79*, 244−254. (b) $^{15}N_2$-thiourea is currently a costly commercial compound, available from Euriso-Top, Gif-sur-Yvette, France.

($SC^{15}N^-$), and at −360 ppm ($^{15}NH_4^+$). The latter signal appeared as a quintet in the H-coupled spectrum with $^1J_{NH} = 91$ Hz. The signal for ammonium appears much more intense than that of the thiocyanate, probably because of a large difference in relaxation times. ^{13}C NMR in water indicated a broad multiplet for the thiocyanate ion at 134 ppm. This might indicate the presence of several species, some of which may not include an ammonium counterion, or alternatively, the presence of small amounts of paramagnetic cations in solution. Therefore, this product was eluted through a short cation exchanger column (Chelex-100, Bio-Rad) loaded with $^{15}NH_4Cl$. This time, the ^{13}C NMR spectrum showed a sharp doublet for $SC^{15}N^-$, with $^1J_{CN} = 14$ Hz. ($^{15}N_2$)-Thiourea was obtained upon heating ($^{15}N_2$)-ammonium thiocyanate in a sealed tube at 190 °C for 2 h. The residue, consisting of a mixture of ($^{15}N_2$)-thiourea and ($^{15}N_2$)-ammonium thiocyanate in a ratio of 1:6, was well separated on a silica gel column eluted with $CHCl_3$/EtOAc and detected on TLC as a yellow spot by dipping in $KMnO_4$ solution. The recovered ($^{15}N_2$)-ammonium thiocyanate can be reused. The ^{15}N NMR spectrum of ($^{15}N_2$)-thiourea in acetone showed one singlet at −278 ppm; this signal appeared as a second-order triplet in the H-coupled spectrum with $^1J_{NH} = 91$ Hz.

($^{15}N_4$)-2-SH-4,6-diaminopyrimidine **6**, which is obtained via the Traube synthesis[28b] from the doubly labeled malononitrile and thiourea, serves as a common synthetic key intermediate for the preparation of all three desired adenine analogue prototypes **1**−**3**. The ^{13}C NMR spectrum of pyrimidine **6** in DMSO-d_6, shows the expected signals at 74 and 177 ppm for C5 and C2, respectively; however, a broad multiplet is observed for C4 and C6 at 159 ppm. Upon addition of NaOH to the sample, this multiplet becomes a sharp doublet at 162 ppm. The measured $^1J_{CN}$ value for the exocyclic nitrogens is 18 Hz. The $^1J_{CN}$ with the endocyclic nitrogens is about 1 Hz and is hidden within the signal's width.[31] Addition of NaOH causes downfield shifts of the C2 and C5 signals by 7 and 2.5 ppm, respectively.

The fifth labeled nitrogen, at the C5 position of pyrimidine **6**, was introduced by nitrosation. $Na^{15}NO_2$ in acidic medium was used for electrophilic substitution of the free C5 position.[28b] Product **7**, with all the desired labels, precipitated from the reaction mixture as a dark green solid. This nitroso compound is stable at room temperature for at least 1 year. The ^{13}C NMR spectrum of product **7** in DMF indicates that this compound is nonsymmetrical, as signals for four different carbons are observed instead of the expected three; C4 and C6 carbons appear at 146 and 140 ppm. Likewise, the ^{15}N NMR spectrum showed two different amine signals, at −293 and −298 ppm. This phenomenon is probably due to the known high barrier to rotation of the nitroso group when it is bound to an electron-rich aromatic moiety. [32] In the present case, this barrier may be even higher due to hydrogen bonding to the adjacent amino group.

Pyrimidine **7** was then reduced with RaNi in DMF to gain both desulfurization and reduction of the nitroso function to triamine, **8**, in one step in 43% yield (Scheme 4). The moderate yield of the isolated product, despite the complete conversion, is due to the limited solubility and stability of triaminopyrimidine, **8**. Still, this yield is superior to a two-step reducing procedure, involving first reduction of the nitroso function to amine with $Na_2S_2O_4$ [28b] in 30% yield, followed by RaNi reduction of thiol **9**.[10] An alternative path involving desulfurization of **6**, followed by nitrosation and reduction to get **8**, was also unfruitful due to low yields in the nitrosation step. Finally, cyclization of **8** was affected with diethoxymethyl acetate, DMEA,[7,8] to give ($^{15}N_5$)-adenine, **1**, in 80% yield.

Scheme 4. Synthesis of ($^{15}N_5$)-Adenine 1 and of ($^{15}N_5$)-8-Bromoadenine, 3[a]

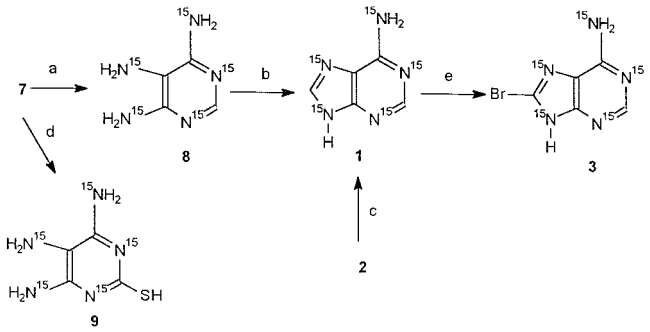

[a] Key: (a) RaNi/DMF/rt/overnight, 43%; (b) DEMA, 80%; (c) RaNi/1 N NaOH/reflux/2 h, 25%; (d) $Na_2S_2O_4/H_2O$/reflux/2 min, 30%; (e) Br_2/H_2O/RT/overnight, 83%.

Scheme 5. Synthesis of ($^{15}N_5$)-2-Hexylthioether-adenine 2[a]

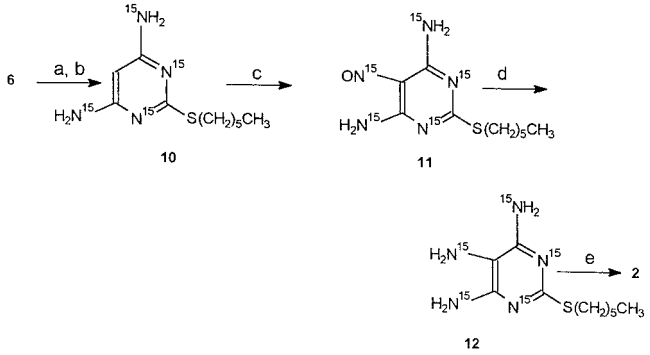

[a] Key: (a) 0.25 M NaOH/MeOH/rt; (b) $Br(CH_2)_5CH_3$/DMF/rt, 89%; (c) $Na^{15}NO_2$/HOAc−H_2O/rt/5 min, 62%; (d) H_2 (1 atm)/PtO_2/EtOH/rt/3 h, 100%; (e) $HCONH_2$, reflux, 1 h, 85%.

The synthesis of ($^{15}N_5$)-2-hexylthioadenine, **2**, involved S-alkylation of pyrimidine **6**, prior to the nitrosation step (Scheme 5), to get a chloroform-soluble pyrimidine derivative **10**, which is convenient for workup procedures and for recovery from NMR samples. Selective S-alkylation was obtained upon treating pyrimidine **6** with NaOH in a methanolic solution at room temperature, freeze-drying, and adding hexyl bromide in DMF. Nitrosation of **10** was achieved with $Na^{15}NO_2$ in aqueous acetic acid within 5 min. The light blue product precipitated from the reaction mixture and was reduced in a quantitative yield by catalytic hydrogenation over PtO_2 at atmospheric pressure. This nitroso reduction is superior to the commonly used sodium dithionate[28b] or Zn[33a] reductions that result in low yields. ($^{15}N_5$)-2-hexylthioadenine, **2**, was obtained from **12** in 85% yield upon cyclization with trimethylorthoformate;[33a] alternatively, cyclization is

(31) Kainosho, M. Caution in using ^{15}N-^{13}C spin−spin coupling for determining (bio)synthetic pathways. *J. Am. Chem. Soc.* **1979**, *101*, 1031−1032. Sethi, S. K.; Gupta, S. P.; Jenkins, E. E.; Whitehead, C. W.; Townsend, L. B.; McCloskey, J. A. Mass spectrometry of nucleic acid constituents. Electron ionization spectra of selectively labeled adenines. *J. Am. Chem. Soc.* **1982**, *104*, 3349−3353.

(32) Oki, M. *Applications of dynamic NMR spectroscopy to organic chemistry*; VCH: Deerfield Beach, FL, 1985; p 83−85.

achieved with formamide to obtain **2** in 80% yield.[33b] ^{15}N NMR spectra of intermediates **10**−**12**, in MeOH at room temperature, are shown in Figure 1. The unsymmetrical nature of intermediate **11** is demonstrated in Figure 1B, as was also observed for intermediate **7**.

The procedures involving 2-thioether heterocycles **10**−**12**, which are MeOH- or $CHCl_3$-soluble, are convenient and result in high yields. Therefore, we considered **2** also as an entry for ($^{15}N_5$)-adenine **1**, which is expected to be obtained upon RaNi reduction of **2**. Complete conversion of **2** to **1** was indeed achieved with RaNi in 1 N NaOH solution at 100 °C for 2 h. However, difficult workup reduced the isolated yield considerably (Scheme 4).

A third adenine prototype, 8-Br-($^{15}N_5$)-adenine, **3**, was obtained in 83% yield upon bromination of **1** in water at room temperature[34] (Scheme 4). This procedure was far superior to bromination in acetic acid[35a] or acetate buffer.[35b]

^{15}N NMR Spectra of Adenine Derivatives. ^{15}N NMR chemical shifts measured for adenine derivatives **1**−**3** (0.07−0.2 M solutions), at room temperature over 30 min at 60.8 MHz, are presented in Table 1 and Figures 2, 4, and 5.

The ^{15}N NMR spectrum of ^{15}N-enriched adenine (**1**), in DMSO-d_6 at room temperature, is shown in Figure 2A. As expected, five signals can be seen, with the high-field triplet clearly corresponding to the NH_2 group. Three of the other peaks are significantly broadened. When the ^{15}N NMR spectrum of adenine was measured with severe exclusion of traces of paramagnetic metal ions (i.e., treatment of NMR tube with nitric acid and EDTA and filtration of DMSO through Chelex-100 resin), no sharpening of those peaks was observed. Namely, this phenomenon indicates that a dynamic process, probably tautomerization, is active.

To unambiguously assign each nitrogen to a specific resonance, we prepared a saturated solution of commercial adenine in DMSO-d_6 (ca. 0.5 M). The ^1H spectrum for this sample shows two lines, at δ 8.15 and 8.17 (these small downfield shifts relative to the ^{15}N-labeled adenine, Figure 2C, are probably due to the increase of 1 order of magnitude of the concentration, which brings about more self-association and base pairing[36]); the higher field of these is some 2 Hz broader. ^{13}C satellites are easily identified, and the observed $^1J_{CH}$ values are 209.4 and 197.3 Hz, respectively. Next, we measured two ^{13}C spectra: 1D and HMBC (2D, long-range ^1H-correlated, gradient assisted). The highest-field of the carbon peaks (δ 118.36), which is obviously C5, had an interaction only with the highest field of the two protons, indicating this to be H8. The other observed cross-peaks fully confirm the carbon assignment of Chenon et al.[37] Most carbon lines are broadened (only C2 is sharp; for the others, $\nu_{1/2}$ is 100−150 Hz). Interestingly, even at 80 °C the signals for carbons 4 and 5 remain quite broad ($\nu_{1/2} \approx 100$ Hz), indicating that the population of the minor tautomer increases with temperature and/or that the process has a large negative entropy of activation (vide infra).

The ^1H NMR spectrum of ^{15}N-enriched adenine, in DMSO-d_6 and at room temperature, is shown in Figure 2C (see also the Experimental Section). Each of the protons has two larger coupling interactions (10−15 Hz). These are almost certainly $^2J_{NH}$ (H2 with N1 and N3, H8 with N7 and N9) since other nitrogens are four bonds away or more. Indeed, when we measured the ^{15}N-correlated HMBC spectrum of a commercial adenine sample (Figure 3), each of the two protons showed two correlated nitrogens. For H8, N7 and N9 are easily differentiated since N9 is "pyrrole-like" and therefore much more shielded than the other "pyridine-like" nitrogens. N1 and N3 correlate with H2; we can distinguish the two signals by looking at coupling interactions of the sharp N1 signal. Under conditions of proton decoupling, both this nitrogen and the NH_2 give a 5.5 Hz doublet. This is probably the $^2J_{NN}$ interaction between these two nuclei. When protons are not decoupled, N1 shows additionally a 15.5 Hz coupling with H2 (vide supra) and two ca. 3 Hz splittings, almost certainly with the NH_2 protons ($^3J_{NH}$); see Figure 2C. At 80 °C, we cannot locate the peaks for N7 and N9 in the enriched compound (or in the HMBC for the natural abundance one), see Figure 2B. Presumably, they are broadened into the noisy baseline. Like in the ^{13}C case, this indicates that even at this temperature, the ^{15}N spectrum has not reached the fast equilibrium limit.

We feel that the above constitutes an unambiguous assignment of the nitrogen signals of adenine, **1**. The nitrogen chemical shifts for this compound were reported in a pioneering study in 1983 by Gonnella et al.[3b] These authors obtained a natural abundance spectrum and assigned the relatively closely spaced signals for N1, N3, and N7 by synthesising isotopomers specifically ^{15}N enriched at each of these three positions. For comparison purposes, we have brought the ^{15}N chemical shifts from both sources in Table 1. The chemical shifts from the 1983 paper have been corrected by 6 ppm to account for the fact that 0.1M $D^{15}NO_3$ was used as an external standard, and negative signs added. The agreement between the two sets of measurements is excellent for N1, N3, and the NH_2, but not so for N7 and N9; significantly, the former nitrogen is shielded, while the latter is deshielded in the Gonnella paper. This may be explained as follows: (1) N7-H−N9-H tautomeric equilibrium is reflected in the chemical shifts of N7 and N9. A smaller $\Delta\delta$ value for these indicates that the tautomer mix is enriched in the N7-H species. While we cannot be sure of the reason for this, it is possible that this is due to the temperature difference between the measurements

(33) (a) Leonard, N. J.; Henderson, T. R. Purine ring rearrangements leading to the development of cytokinin activity. Mechanism of the rearrangement of 3-benzyladenine to N^6-benzyladenine. *J. Am. Chem. Soc.* **1975**, *97*, 4990−4999. (b) Robins, R. K.; Dille, K. J.; Willits, C. H.; Christensen, B. E. Purines. II. The synthesis of certain purines and the cyclization of several substituted 4,5-diaminopyrimidines. *J. Am. Chem. Soc.* **1953**, *75*, 263−266.

(34) Holy, A.; Kohoutova, J.; Merta, A.; Votruba, I. 9-(Aminoalkyl)-8-hydroxyadenines: Preparation, mechanism of formation and use in affinity chromatography of S-adenosyl-L-homocysteine hydrolase. *Collect. Czech. Chem. Commun.* **1986**, *51*, 459−477.

(35) (a) Seela, F.; Wei, C.; Kazimierczuk, Z. 138. Substitutent reactivity and tautomerism of isoguanosine and related nucleosides. *Helv. Chim. Acta* **1995**, *78*, 1843−1854. (b) Ikehara, M.; Kneko, M. Studies of nucleosides and nucleotides- XLI. Purines cyclonucleosides-8. Selective sulfonylation of 8-bromoadenosine derivatives and an alternate synthesis of 8,2′- and 8,3′-S-cyclonucleosides. *Tetrahedron* **1970**, *26*, 4251−4259.

(36) Dyllick-Brenzinger, C.; Sullivan, G. R.; Pang, P. P.; Roberts, J. D. Self-association and base pairing of guanosine, cytidine, adenosine, and uridine in dimethyl sulfoxide solution measured by ^{15}N nuclear magnetic resonance spectroscopy. *Proc. Natl. Acad. Sci. U.S.A.* **1980**, *7*, 5580−5582.

(37) Chenon, M.-T.; Pugmire, R. J.; Grant, D. M.; Panzica, R. P.; Townsend, L. B. Carbon-13 magnetic resonance. XXVI. A quantitative determination of the tautomeric populations of certain purines. *J. Am. Chem. Soc.* **1975**, *97*, 4636−4642.

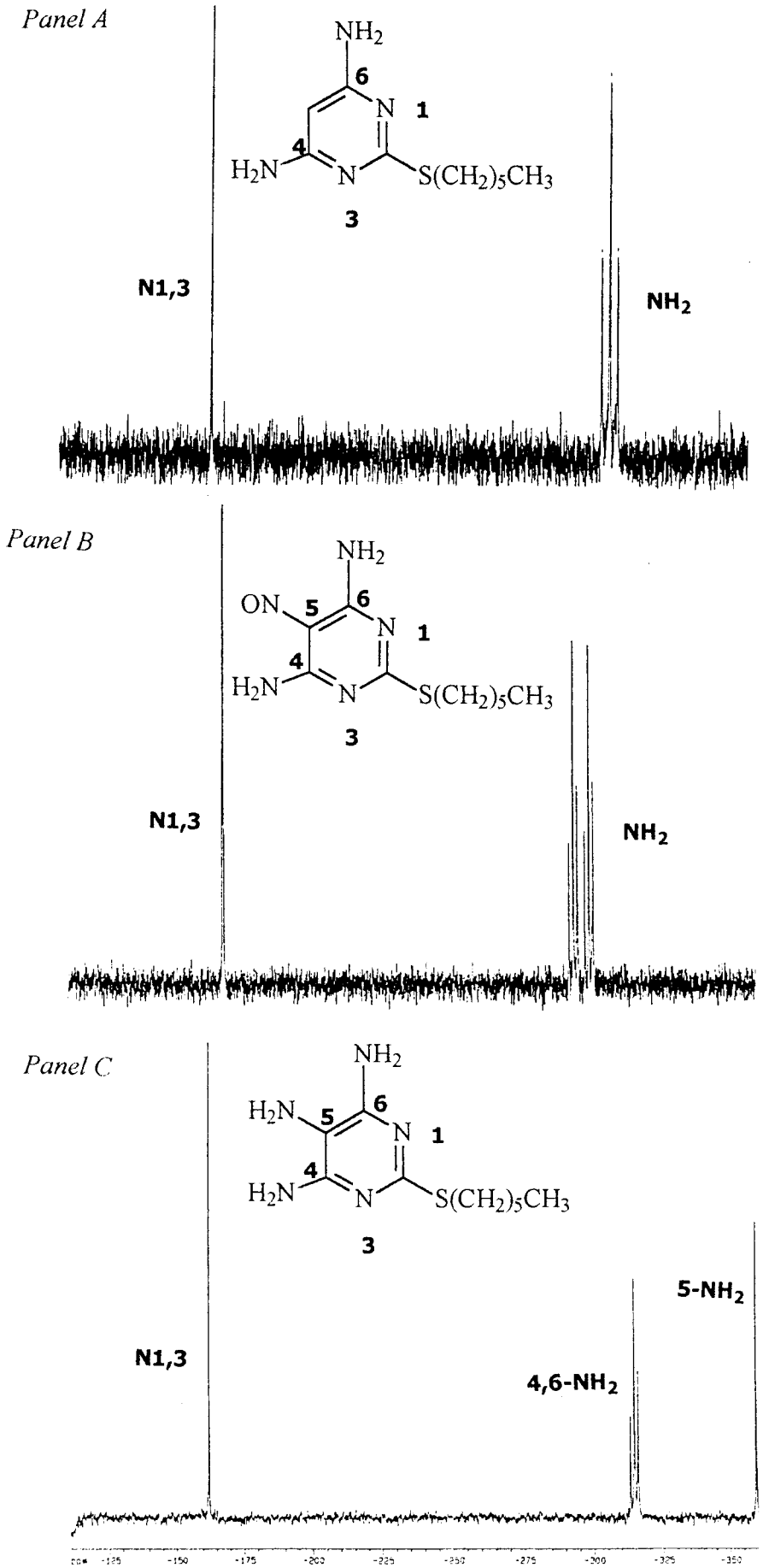

Figure 1. ^{15}N NMR spectra of compounds **10**, **11**, and **12**, panels A, B, and C, respectively. Measured at 30.4 MHz (A) and at 60.8 MHz (B, C) at 25 °C in MeOH. Panel B, unlike panels A and C, reveals a nonsymmetrical compound.

Table 1. ^{15}N NMR Chemical Shifts for Compounds 1−3

adenine derivative	solvent	*T* (°C)	N1	N3	N7	N9	NH_2
1	DMSO	25	−145.7	−151.5	−140.3	−222.6	−301.2
1[a]	DMSO	50	−146[a]	−151[a]	−154[a]	−212[a]	−302[a]
2	DMSO	25	−154.5	−163.4	−140.3	−225.0	−300.3
2	MeOH[b]	25	−157.3	−165.7	−152.0	−226.0	−308.1
2	MeOH[c]	−53	−161.0	−168.5	−153.3	−226.2	−304.7
3	DMSO[d]	77	−144.8	−151.5	−139.4	−224.2	−305.1

[a] Reference 3b. [b] In 100% CD_3OD. Spectrum not shown. [c] 9:1 CH_3OH + CD_3OD. [d] Spectrum not shown.

(50[3b] vs 25 °C). The population of the minor tautomer apparently increases with temperature. (2) An alternative or additional reason is hinted in Gonella's report that the $\Delta\delta$ value for these nitrogens is 43 ppm in water and 56 ppm in DMSO (and 80−85 ppm in DMSO, in our hands). As shown in Table 1, the chemical shift of N7 is significantly effected by interactions with an H-bonding solvent. Therefore, it is possible that the DMSO we used contained less water, since small amounts of extra water maybe enough to affect the tautomeric equilibrium.

Significant changes in the nitrogen chemical shifts due to purine ring substitution with 2-thioether group are observed (Table 1). Most pronounced are the changes in the N1 and N3 signals that are shifted upfield by 7 and 12 ppm, respectively, due to resonance effects of the thioether group. Changes in the chemical shifts due to 8-Br substitution are minor (ca. 1 ppm) and are observed for N7, N9, and NH_2.

Differences in the chemical shifts due to interactions with the solvent are most pronounced for N7. For instance, N7 of 2-hexylthioether-adenine appears at 140 ppm in DMSO but shifts 12 ppm upfield in MeOH due to H-bonding interactions with the latter solvent[38] (Table 1).

The effects of the adenine ring substitutions on the ^{13}C NMR spectra of compounds **2** and **3** are shown in Table 2.

Indication of Tautomeric Equilibria of Adenine Derivatives 1−3 Based on ^{15}N NMR Spectra. Adenine has 12 possible tautomeric structures (Scheme 6). Each tautomer has a specific H-bonding donor and acceptor pattern, which may determine molecular recognition. Therefore, the possible effects of electron-withdrawing/donating groups at C8 and C2 positions of the adenine on the relative stability of these tautomers were investigated with ^{15}N NMR and quantum mechanical calculations.

For spectra below coalescence, a dynamic process-induced broadening of lines is proportional to the square of the magnetic field. Therefore, for observing dynamic processes, high-field NMR machines may be necessary. The combination of a high-field NMR machine with 100% ^{15}N-enrichment at all positions of adenine and its derivatives, yielded high-quality spectra. These spectra enabled an insight into the tautomeric equilibria of adenine derivatives in solution, based on the line-width of the signals (Figures 2, 4, and 5).

The ^{15}N NMR spectrum of adenosine-5′-monophosphate (AMP), shows sharp signals for all of the adenine ring nitrogens (Figure 6). The NMR signals can be divided into three groups according to their ^{15}N chemical shift and their chemical character: (1) the N^6-amine at highest field, (2) N9, which is a ring nitrogen of amine character, at ca. −210 ppm, and (3) N1, N3, and N7 ring nitrogens, of imine character, at −150 to −170 ppm.[3a,b] In contrast, the spectrum of ($^{15}N_5$)-adenine in DMSO at room temperature (Figure 2A) shows broadening of some of the signals, indicating a mixture of more than one species in dynamic equilibrium, probably tautomers. Since there is only one set of signals (fast exchange regime), we cannot directly deduce the chemical shifts of the equilibrating species; however, the width of individual peaks is related to the square of chemical shift difference between them. Therefore, a sharp line indicates that the ^{15}N shifts of the species are very similar; a broad line indicates larger $\Delta\delta$ values.

Indeed, the N^6 signal is expected to be sharp since the N^6-amino tautomers, and not the imino tautomers, are the most dominant, with less than 0.001% population estimated for the imino tautomers in a variety of solvents.[39] This is confirmed by the fact that N^6 appears as a triplet proving that its two connected nitrogens do not participate in the exchange process. The N1 signal is also sharp, suggesting that this nitrogen has an imine character in all populated tautomers (i.e., this nitrogen appears in a narrow range of chemical shifts).

In contrast, N3, N7, and N9 are much broader, indicating that the prototropic tautomerism equilibrium involves species in which these nitrogens exist in the amino form. N9 is still shielded relative to the other ring nitrogens, showing that the N9-H tautomer is dominant.

However, the participation of the adenine N3 in the prototropic tautomerism equilibrium, in addition to N7 and N9, was rather unexpected on the basis of the following reported experimental results and theoretical calculations, which suggest N9-H as the major tautomer and N7-H as the minor one.

Previous reports claimed that adenine in polar solutions exists as a mixture of only two amino tautomers—the N9-H and N7-H isomers.[37,39−42] In an aqueous solution, the N9-H tautomer predominates over the N7-H form by a factor of 4.[43] Infrared spectra of matrix-isolated adenine and its ^{15}N isotopomers with ^{15}N at the N9 or N7 positions provided evidence that the amino-N9-H

(38) Cho, B. P.; Evans, F. E. Structure of oxidatively damaged nucleic acid adducts. 3. Tautomerism, ionization and protonation of 8-hydroxyadenosine studied by ^{15}N NMR spectroscopy. *Nucleic Acids Res.* **1991**, *19*, 1041−1047.

(39) (a) Wolfenden, R. V. Tautomeric equilibria in inosine and adenosine. *J. Mol. Biol.* **1969**, *40*, 307−310. (b) Schumacher, M.; Gunther, H. ^{13}C, ^{1}H Spin−spin coupling. 9. Purine. *J. Am. Chem. Soc.* **1982**, *104*, 4167−4173.

(40) Dreyfus, M.; Dodin, G.; Bensaude, O.; Dubois, J. E. Tautomerism of purines. I. N(7)H⇌N(9)H equilibrium in adenine. *J. Am. Chem. Soc.* **1975**, *97*, 2369−2376.

(41) (a) Shugar, D.; Psoda, A. In *Landolt-Bornstein-New Series: Biophysics of Nucleic Acids*; Saenger, W., Ed.; Springer: Berlin; Vol. VII/1d. (b) Kwiatkowski, J. S.; Person, W. B. In *Theoretical Biochemistry and Molecular Biophysics*; Beveridge, D. L., Lavery, R., Eds.; Adenine Press: Guiderland, NY, 1990; Vol. 1: DNA, p 153. (c) Elguero, J.; Marzin, C.; Katritzky, A. R.; Linda, P. In Adv*ances in Heterocyclic Chemistry, Supplement I*; Katrizky, A. R., Bouton, A. J., Eds.; Academic Press: New York, 1976. (d) Kwiatkowski, J. S.; Pullman, B. Tautomerism and electronic structure of biological pyrimidines. *Adv. Heterocycl. Chem.* **1975**, *18*, 199−335.

(42) (a) Eastman, J. W. The fluorescence and tautomerism of adenine. *Ber. Bunsen-Ges. Phys. Chem.* **1969**, *73*, 407−412. (b) Laawley, P. D. In *Fused Pyrimidines*; Brown, D. J., Ed.; Wiely: New York, 1971; p 439. (c) Gonella, N. C.; Roberts, J. D. Studies of the tautomerism of purine and the protonation of purine and its 7-and 9-methyl derivatives by nitrogen-15 nuclear magnetic resonance. *J. Am. Chem. Soc.* **1982**, *104*, 3162−3164. (d) Pugmire, R. J.; Grant, D. M. Carbon-13 magnetic resonance. XIX. Benzimidazole, purine, and their anionic and cationic species. *J. Am. Chem. Soc.* **1971**, *93*, 1880−1886. (e) Reddy, G. S.; Mandell, L. Goldstein, J. H. The preparation and nuclear magnetic resonance spectra of the *N*-acetyl derivatives of imidazoles, benzimidazoles, and purines. *J. Chem. Soc.* **1963**, 1414−1421.

(43) Reference 41a, p 308.

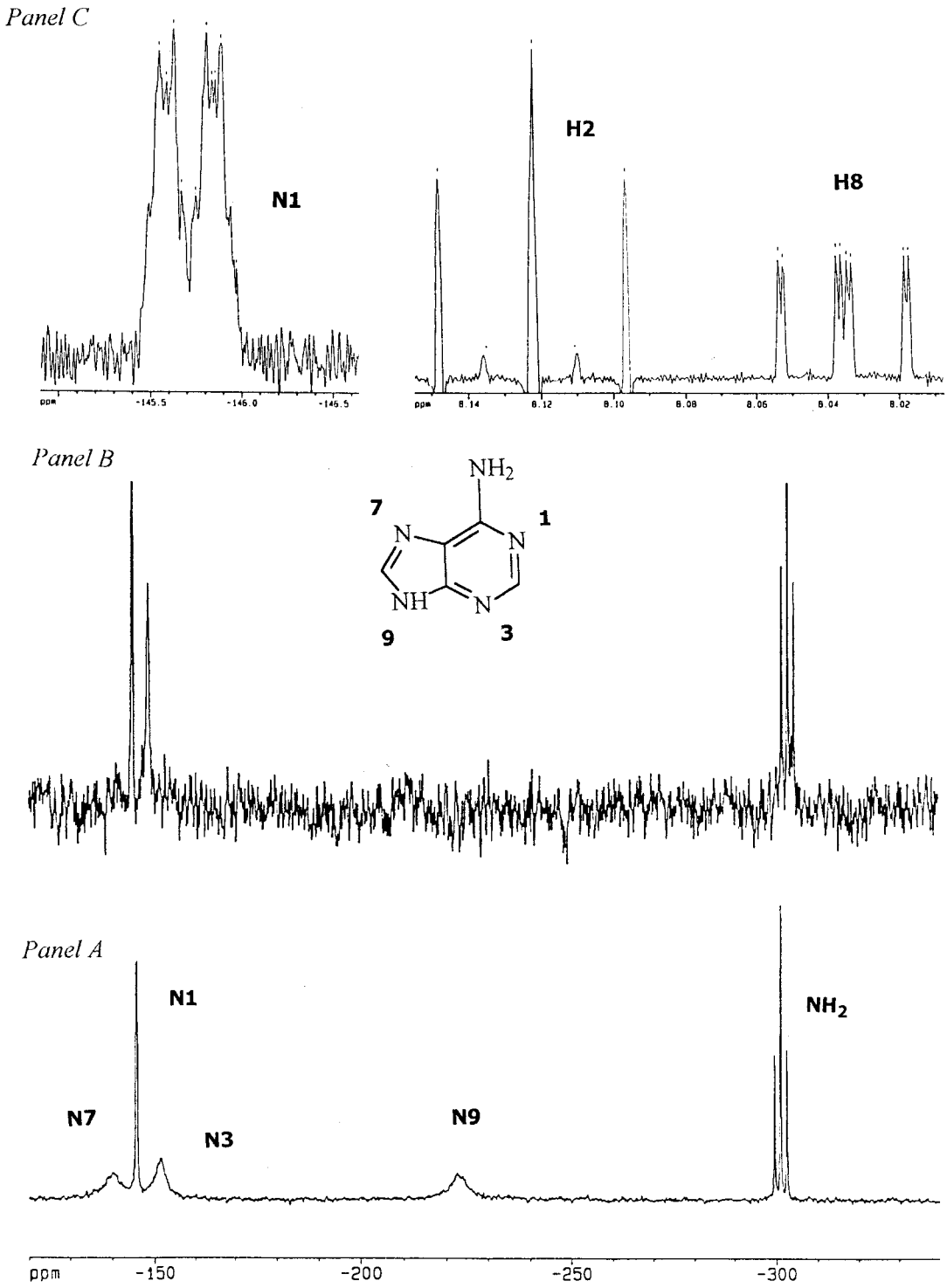

Figure 2. ^{15}N NMR spectra of compound **1** measured at 60.8 MHz in DMSO. Panel A: at 25 °C. Panel B: at 80 °C. Panel C: H-coupled signal of N1 and N-coupled signals of H2 and H8.

tautomer of adenine strongly dominates in low-temperature inert-matrixes, simulating gas-phase conditions. The greater stability of the N7-H tautomer in polar media is explained by it having a larger dipole moment than the N9-H tautomer and, hence, can be more strongly stabilized in polar media. Consequently, the N7-H form should have a less favorable relative energy in an inert environment.[44] N9-H is the highly dominant tautomer also for isolated molecules of purine and 2-Cl-adenine in a noninteracting environment, deduced from the combined IR matrix isolation and ab initio studies.[45] This has also been proven by the microwave spectrum of adenine in a continuous wave seeded supersonic beam combined with ab initio calculations.[46]

(44) Nowak, M. J.; Lapinski, A.; Kwiatkowski, J. S.; Leszczynski, J. Molecular structure and infrared spectra of adenine. Experimental matrix isolation and density functional theory study of adenine 15N isotopomers. *J. Phys. Chem*. **1996**, *100*, 3527−3534.

(45) Nowak, M. J.; Rostkowska, H.; Lapinski, A.; Kwiatkowski, J. S.; Leszczynski, J. Tautomerism N9H−N7H of purine, adenine, and 2-chloroadenine: combined experimental IR matrix isolation and ab initio quantum mechanical studies. *J. Phys. Chem*. **1994**, *98*, 2813−2816.

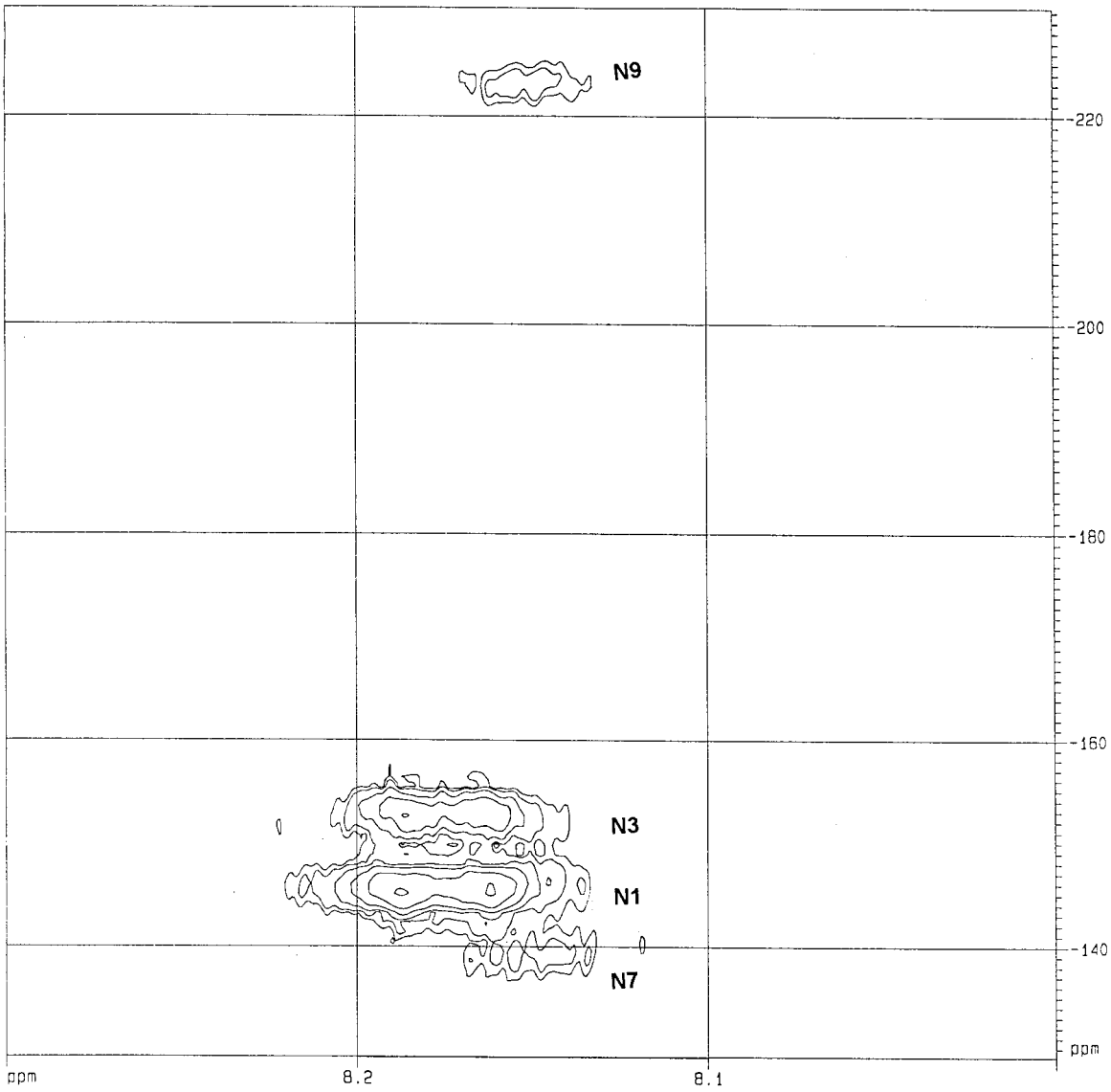

Figure 3. ^{15}N-correlated HMBC spectrum of adenine at natural abundance in DMSO at 25 °C.

Table 2. ^{13}C NMR Chemical Shifts for Compounds 1−3 at 25 °C

adenine derivative	solvent	C2	C4	C5	C6	C8
1	DMSO	152.4	151.2	118.3	155.1	139.3
2	MeOH	166.6	150.3	116.0	155.9	139.8
3	DMSO	147.8	150.8	118.6	150.8	127.5

The existence of 15% or 19% of N7-H tautomer in adenine DMSO solution was proposed based on ^{13}C chemical shifts[37] or ^{13}C,H spin−spin coupling,[39b] respectively. About 22% of N7-H tautomer in aqueous solution was reported on the basis of a temperature jump relaxation experiment,[40] and 13.5% of this tautomer was estimated to be present in DMSO based on ^{15}N NMR data.[3b] The predominance of the N9-H vs the N7-H tautomer is explained by the repulsion between lone pairs of N3 and N9, in the N7-H tautomer.[3b] Steric hindrance between N7-H and N^6-amine is yet another reason for the low population of this tautomer, based on the fact that in purine the ratio between N9-H and N7-H tautomers is 60:40, whereas in adenine the ratio is 85:15.[37] In tautomer N7-H, the N^6-amine adopts an out-of-plane conformation to avoid this steric hindrance; a conformation which is energetically unfavorable. Although for the N3-H tautomer, there are no unfavorable interactions such as repulsion of nonbonding electron pairs or steric hindrance with N^6 amine, this tautomer has been seldom considered in the literature, and no evidence has been provided before for its existence in solution. The first evidence of the existence of the N3-H amino tautomer was mentioned in a combined matrix-isolation FT-IR and ab initio study.[47]

The spectrum of compound **2** in DMSO at room temperature (Figure 4A) was similar to that of adenine (Figure 2A); however, the N3, N7, and N9 lines are relatively sharper. In MeOH, containing 10% CD_3OD, at 0 °C (Figure 4B), a less viscous medium than DMSO, the N7 and N9 lines are not observed, again (vide supra) due to slow relaxation. This is supported by the spectrum in

(46) Brown, R. D.; Godfrey, P. D.; McNaughton, D.; Pierlot, A. P. A study of the major gas-phase tautomer of adenine by microwave spectroscopy. *Chem. Phys. Lett.* **1989**, *156*, 61−63.

(47) Houben, L.; Schoone, K.; Smets, J.; Adamowicz, L.; Maes, G. Combined matrix-isolation FT-IR and ab initio 6-31++G** studies on tautomeric properties of nucleic acid bases and simpler model molecules. *J. Mol. Struct.* **1997**, *410−411*, 397−401.

Scheme 6. Tautomers of Adenine Derivatives

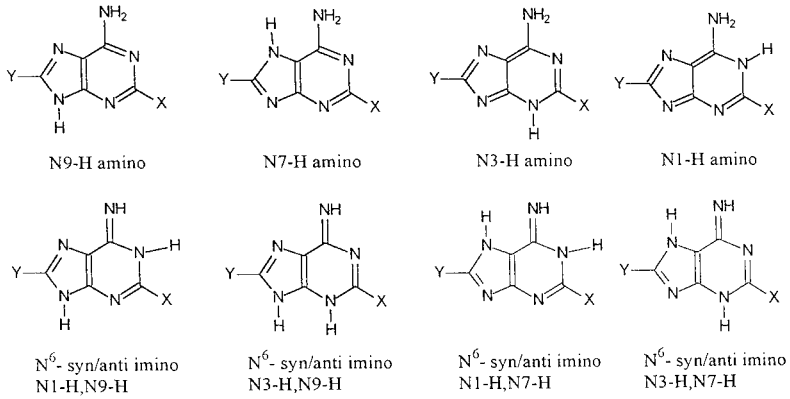

MeOH at −53 °C (Figure 4C), where these three nitrogen signals are again visible as broad lines.[48]

Line-broadening of N9, N7, and N3 was observed also for 8-Br-adenine in DMSO solution (Figure 5), although less significant than for adenine (Figure 2A).

In view of the above results, analysis of the population of the relevant tautomers, for instance by line-shape-analysis, was impossible. Such a calculation would necessitate obtaining spectra below the coalescence temperature of the nitrogen lines in order to observe separate lines for each exchanging species. DMSO solutions cannot be cooled much below room temperature; **1** and **3** proved to be too insoluble in MeOH, while **2** precipitated out of solution at −63 °C (below the temperature at which we measured spectrum 4C).

The practical limitations of the ^{15}N NMR spectral measurements of adenine derivatives encouraged us to address the question of the relative stability of N3-H, N7-H, and N9-H tautomers by theoretical calculations.

Studies of Tautomeric Equilibria of Adenine Derivatives 1−3 Based on Quantum Mechanical Calculations. Several theoretical studies dealt with the tautomerism of adenine and its derivatives.[49−51]

Early computational studies of the tautomerism in adenine predicted the N9-H tautomer to be the most stable in the gas phase, followed by the N7-H tautomer. All other 10 tautomers were predicted to be considerably less stable. However, due to the available methods and computational resources at the time, these studies used either semiempirical [49a−c] or low-level ab initio[49d,e] calculations. Solvent effects were included only at the semiempirical level.[49c] Recently, correlation effects were included in a study of all the tautomers of adenine, but in this case solvent effects were not included.[50] This led to the perception that adenine exists only in the N9-H and N7-H tautomeric forms in solution. Therefore, later studies on adenine tautomerism considered mainly the N9-H and N7-H isomerism.[44,45,51]

However, correlation effects are essential to describe the differences in charge distribution in the gas phase for the various isomers of adenine. Thus, we performed quantum mechanical (QM) calculations to investigate the tautomeric equilibria of adenine, 2-MeS-adenine, and 8-Br-adenine using density functional theory (DFT) and second-order perturbation theory methods. DFT calculations were performed using the B3LYP functional[52] and perturbation theory calculations were performed using MP2.[53] These methods were chosen together with the Pople 6-31G(d)[54] and 6-311+G(2df,2p)[55] basis sets. Additionaly, B3LYP calculations were calculated with the Dunning cc-pVTZ[56] basis set augmented with diffuse functions. Only the highest level results are shown.

(48) Signals for N7 and N9 could be observed in the spectrum of **2** in 100% CD_3OD solution, due to exchange of N7-H and N9-H with deuterium. J_{ND} is 6.5 times smaller than J_{NH}.

(49) (a) Pullman, B.; Berthod, H.; Dreyfus, M. Amine-imine tautomerism in adenines. *Theor. Chim. Acta (Berlin)* **1969**, *15*, 265−268. (b) Norinder, U. A theoretical reinvestigation of the nucleic bases adenine, guanine, cytosine, thymine and uracil using AM1. *THEOCHEM* **1987**, *151*, 259−269. (c) Katritzky, A. R.; Karelson, M. AM1 calculations of reaction field effects on the tautomeric equilibria of nucleic acid pyrimidine and purine bases and their 1-methyl analogues. *J. Am. Chem. Soc.* **1991**, *113*, 1561−1566. (d) Mely, B.; Pullman, A. Ab initio calculations on cytosine, thymine and adenine. *Theor. Chim. Acta (Berlin)* **1969**, *13*, 278−287. (e) Sabio, M.; Topiol, S.; Lumma, W. C., Jr. An investigation of tautomerism in adenine and guanine. *J. Phys. Chem.* **1990**, *94*, 1366−1372.

(50) Ha, T. K.; Keller, M. J.; Gunde, R.; Gunthard, H. H. Quantum chemical study of structure, energy, rotational constants, electric dipole moments and electric field gradients of all isomeric adenines. *THEOCHEM* **1996**, *364*, 161−181.

(51) Holmen, A.; Broo, A. A theoretical investigation of the solution N(7)H ↔ N(9)H tautomerism of adenine. *Int. J. Quantum Chem.* **1995**, *QBS22*, 113−122.

(52) (a) Lee, C.; Yang, W.; Parr, R. G. Development of the Colle-Salvetti correlation-energy formula into a functional of the electron density. *Phys. Rev.* **1988**, *B 37*, 785−789. (b) Miehlich, B.; Savin, A.; Stoll, H.; Preuss, H. Results obtained with the correlation-energy density functionals of Becke and Lee, Yang and Parr. *Chem. Phys. Lett.* **1989**, *157*, 200−206. (c) Becke, A. D. Density-functional thermochemistry. III. The role of exact exchange. *J. Chem. Phys.* **1993**, *98*, 5648−5652.

(53) Møller, C.; Plesset, M. S. Note on an approximation treatment for many-electron systems. *Phys. Rev.* **1934**, *46*, 618−622.

(54) (a) Ditchfield, R.; Hehre, W. J.; Pople, J. A. Self-consistent molecular orbital methods. IX. An extended Gaussian-type basis for molecular orbital studies of organic molecules. *J. Chem. Phys.* **1971**, *54*, 724−728. (b) Hehre, W. J.; Ditchfield, R.; Pople, J. A. Self-consistent molecular orbital methods. XII. Further extensions of Gaussian type basis sets for use in molecular orbital studies of organic molecules. *J. Chem. Phys.* **1972**, *56*, 2257−2261. (c) Hariharan, P. C.; Pople, J. A. Accuracy of AH_n equilibrium geometries by single determinant molecular orbital theory. *Mol. Phys.* **1974**, *27*, 209−214. (d) Gordon, M. S. The isomers of silacyclopropane. *Chem. Phys. Lett.* **1980**, *76*, 163−168. (e) Hariharan, P. C.; Pople, J. A. The influence of polarization functions on molecular orbital hydrogenation energies. *Theor. Chem. Acta* **1973**, *28*, 213−222. (f) Francl, M. M.; Pietro, W. J.; Hehre, W. J.; Binkley, J. S.; Gordon, M. S.; DeFrees, D. J.; Pople, J. A. Self-consistent molecular orbital methods. XXIII. A polarization-type basis set for second row elements. *J. Chem. Phys.* **1982**, *77*, 3654−3665.

(55) (a) Krishnan, R.; Binkley, J. S.; Seeger, R.; Pople, J. A. Self-consistent molecular orbital methods. XX. A basis set for correlated wave functions. *J. Chem. Phys.* **1980**, *72*, 650−654. (b) McLean, A. D.; Chandler, G. S. Contracted Gaussian basis set for molecular calculations. I. Second row atoms, Z=11−18. *J. Chem. Phys.* **1980**, *72*, 5639−5648. (c) Frisch, M. J.; Pople, J. A.; Binkley, J. S.; Self-consistent molecular orbital methods. 25. Supplementary functions for Gaussian basis sets. *J. Chem. Phys.* **1984**, *80*, 3265−3269. (d) Clark, T.; Chandrasekhar, J.; Spitznagel, G. W.; Schleyer, P. v. R. Efficient diffuse function-augment basis set for anion calculations. III. The 3-21+G basis set for first-row elements, Li−F. *J. Comput. Chem.* **1983**, *4*, 294−301.

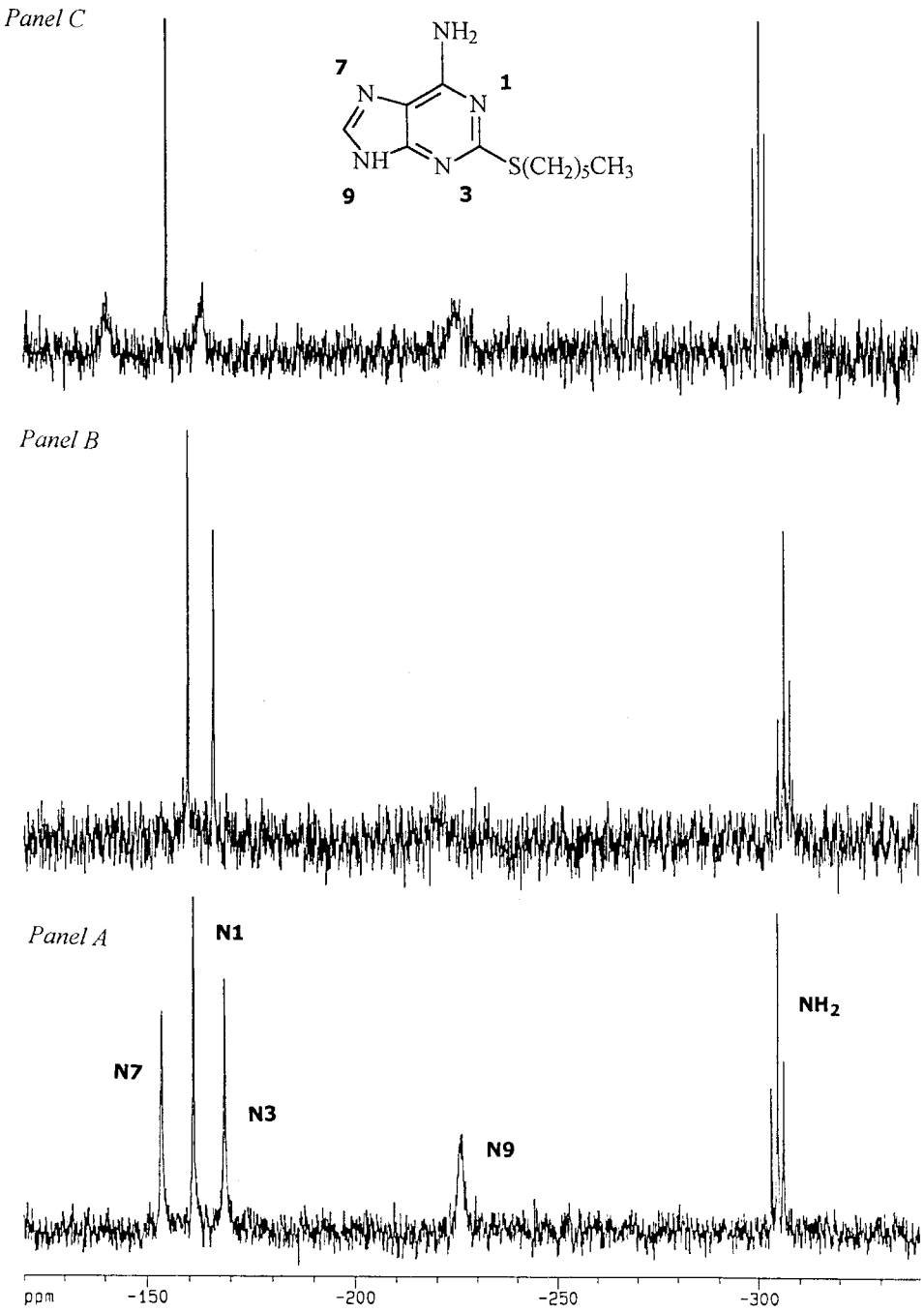

Figure 4. ^{15}N NMR spectra of compound **2**. Panel A: at 25 °C in DMSO. Panel B: at 0 °C in MeOH (containing 10% CD_3OD). Panel C: at −53 °C in MeOH (containing 10% CD_3OD).

In addition to accurate gas-phase calculations, it is necessary to include solvent effects, since interactions of adenine with various solvents influence its tautomeric ratio. Solvent effects were included using two self-consistent reaction field (SCRF) methods: the polarizable continuum model (PCM)[57] combined with B3LYP/6-31G-(d) and the SCRF Poisson−Boltzmann (SCRF-PB)[58] method combined with B3LYP/6-31G(d,p). In addition to the continuum models used, a discrete solvent molecule approach that mimics the first solvation shell effects was employed to investigate the role of specific solute−solvent interactions as well as structural features of the solvent

(56) (a) Dunning, T. H. Gaussian-basis sets for use in correlated molecular calculations. 1. The atoms Boron through Neon and Hydrogen. *J. Chem. Phys.* **1989**, *90*, 1007−1023. (b) Kendall, R. A.; Dunning, T. H.; Harrison, R. J. Electron affinities of the 1st-row atoms revisited − systematic basis-sets and wave functions. *J. Chem. Phys.* **1992**, *96*, 6796−6806. (c) Woon, D. E.; Dunning, T. H. Gaussian-basis sets for use in correlated molecular calculations. 3. The atoms Aluminum through Argon. *J. Phys. Chem.* **1993**, *98*, 1358−1371.

(57) Miertus, S.; Scrocco, E.; Tomasi, J. Electrostatic interaction of a solute with a continuum. A direct utilization of ab initio molecular potentials for the prevision of solvent effects. *Chem. Phys.* **1981**, *55*, 117−129.

(58) (a) Tannor, D. J.; Marten, B.; Murphy, R.; Friesner, R. A.; Sitkoff, D.; Nicholls, A.; Ringnalda, M.; Goddard, W. A., III; Honig, B. Accurate first principles calculation of molecular charge distributions and solvation energies from ab initio quantum mechanics and continuum dielectric theory. *J. Am. Chem. Soc.* **1994**, *116*, 11875−11882. (b) Marten, B.; Kim, K.; Cortis, C.; Friesner, R. A.; Murphy, R. B.; Ringnalda, M. N.; Sitkoff, D.; Honig, B. New model for calculation of solvation free energies: Correction for self-consistent reaction field continuum dielectric theory for short-range hydrogen-bonding effects. *J. Phys. Chem.* **1996**, *100*, 11775−11788.

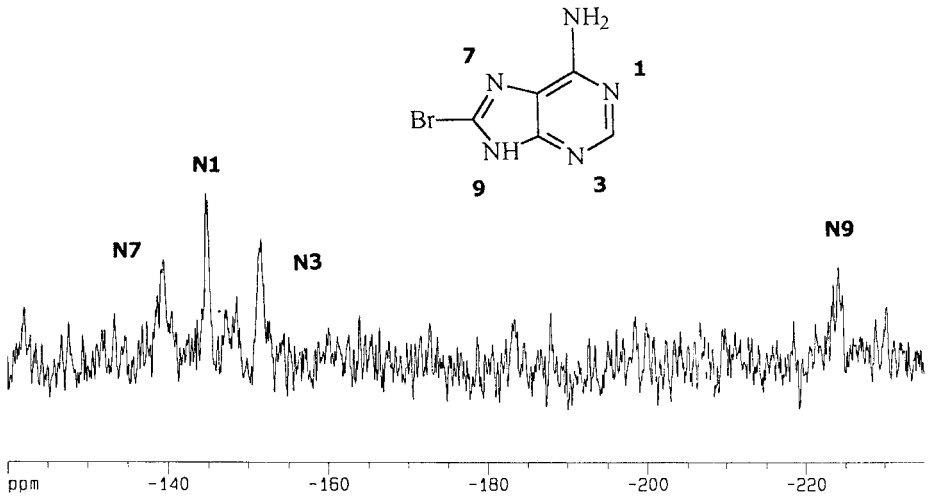

Figure 5. ^{15}N NMR spectrum of compound **3** in DMSO at 25 °C.

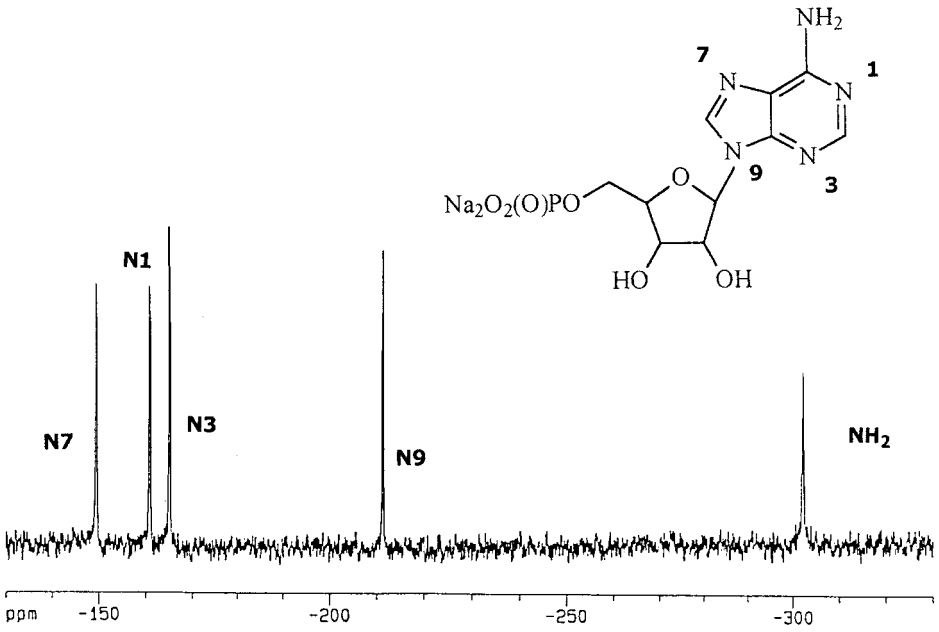

Figure 6. ^{15}N NMR spectrum of AMP in H_2O (pH 5.5) at 25 °C.

on the tautomeric equilibria of adenine and its derivatives. This was performed with DFT calculations on a model supermolecular system that included the adenine solute and three DMSO solvent molecules (Figure 7).

Gas-Phase Tautomerism. We performed a preliminary screening of all 12 tautomers (Scheme 6) of 2-MeS-adenine and 8-Br-adenine using B3LYP/6-31G(d). Previously, all tautomers of adenine were investigated at the MP2/6-31G(d,p) level.[50]

The imino tautomers were found to be more than 12 kcal/mol less stable than the most stable tautomer, the N9-H amino tautomer. Indeed, our ^{15}N NMR data do not indicate the presence of any imino tautomers, but rather a sharp signal for N^6-amine (vide supra). The N1-H amino tautomer was found to be the least stable amino isomer, by more than 12 kcal/mol relative to the N9-H tautomer. This result is illustrated by ^{15}N NMR spectra of these compounds, which show a sharp signal for N1 (Figures 2 and 4).

Thus, only the three most stable amino tautomers, namely, N9-H, N7-H, and N3-H, were further considered at higher level calculations.

Inspection of the results in Table 3 reveals that the N9-H tautomer is the most stable isomer in the gas phase for adenine and the 2-MeS- and 8-Br-adenine derivatives. In the case of adenine, the N7-H and N3-H tautomers are more than 7 kcal/mol less stable than the N9-H isomer. The reason for the preference for the N9-H tautomer is probably possible attractive interaction between N7 and N^6-NH_2; N3 and N9-H, and N1 and N^6-NH_2.[50] Moreover, the N7-H isomer is less favorable because of repulsion between the N7-H and the adjacent N^6-amino hydrogen. Indeed, examination of the geometry of the N7-H tautomer revealed that the N7-H and the adjacent N^6-amino hydrogen are distorted out-of-plane to avoid a repulsive interaction, leading to an energetically unfavorable conformation. The N9-H tautomer also seems to have more favorable conjugation between the exocyclic amino group and the purine moiety than the N7-H form, as inspection of resonance structures may reveal. For the N3-H isomer, there are no unfavorable interactions such as repulsion of nonbonding electron-pairs or steric hindrance with N^6-amino hydrogens. On the other hand, stabilizing intramolecular interactions

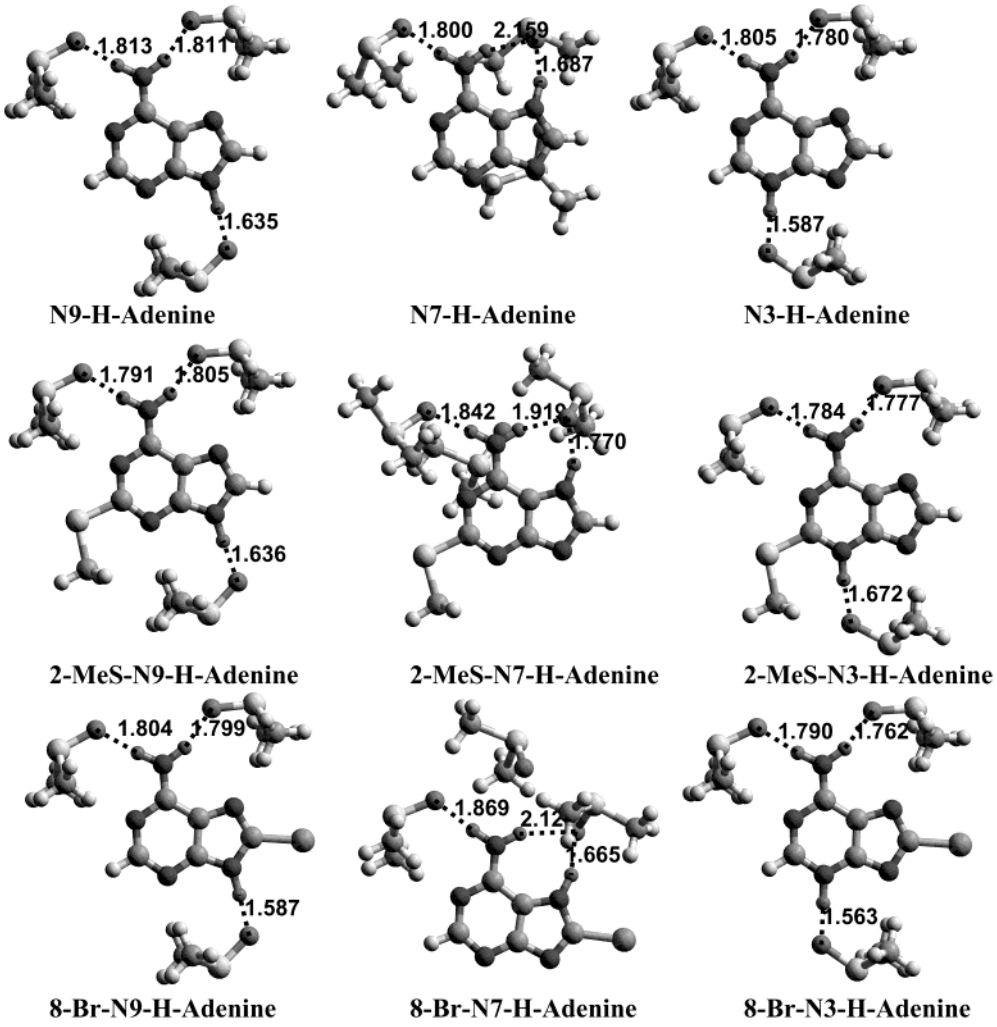

Figure 7. Most stable supermolecule conformers of the N9-H, N7-H, and N9-H tautomers of adenine, 2-MeS-adenine, and 8-Br-adenine.

Table 3. Relative Free Energies, $\Delta G^{tautomer}$, and Dipole Moments, μ, of Adenine (Ad), 2-MeS-adenine (2-MeS-Ad), and 8-Br-adenine (8-Br-Ad) Amino Tautomers in the Gas Phase

	$\Delta G^{tautomer}$ (kcal/mol)			μ (D)
	B3LYP/6-311+ G(2df,2p)[a]	MP2/6-311+ G(2df,2p)[a]	B3LYP/Aug-cc-pVTZ[a]	B3LYP/ 6-31G(d)
Ad-9H	0	0	0	2.45
Ad-7H	7.82	7.59	7.79	6.74
Ad-3H	7.39	7.45	7.36	4.09
2-MeS-Ad-9H	0	0	0	3.32
2-MeS-Ad-7H	7.45	7.24	7.45	6.13
2-MeS-Ad-3H	8.64	8.63	8.76	5.53
8-Br-Ad-9H	0	0	0	1.20
8-Br-Ad-7*H*	7.72	7.38	7.65	6.93
8-Br-Ad-3*H*	5.13	5.02	5.10	5.69

[a] All tautomers were optimized at the B3LYP/6-31G(d) level. Thermal corrections included.

are possible. For 2-MeS-adenine the N3-H-isomer, is the least stable of the three tautomers, being 8.8 kcal/mol less stable than the N9-H tautomer, while the N7-H tautomer is 7.5 kcal/mol less stable. On the other hand, for 8-Br-adenine the N3-H tautomer is only 5.1 kcal/mol less stable than 8-Br-9H-adenine, while the energy gap between the N7-H isomer and 8-Br-9H-adenine is 7.7 kcal/mol. Thus, it appears that the 2-thioether substitution destabilizes the N3-H isomer whereas the 8-bromo substitution destabilizes the N7-H and N9-H isomers in the gas phase.

In conclusion, it seems clear that in the gas phase only the N9-H tautomer contributes to the population of tautomers. The fact that two inherently different QM methods, density functional theory (B3LYP) and second-order perturbation theory (MP2), gave very similar results with large basis sets adds confidence to the results.

Solution-Phase Tautomerism. To explain the ^{15}N NMR data obtained for adenine and its derivatives in DMSO solution, we included solvent effects to evaluate the relative stability of the most stable tautomers in the solution phase. First, free energies of solvation in DMSO were calculated using two self-consistent reaction field (SCRF) models: The polarizable continuum model (PCM)[57] and the SCRF Poisson−Boltzmann (SCRF-PB)[58] model. Thereafter, the energy of solvation was estimated using an approach that treats the tautomer and specific H-bonding DMSO molecules as a supermolecule (Figure 7). The use of two inherently different approaches to solvation, namely continuum and discrete, adds considerable confidence to the computational results as these approaches are complementary.

The use of continuum models to describe solvation of biologically important molecules is well established.[59] However, it is clear that continuum models, by definition

(in the Laplace and Poisson equations), can only account for electrostatic effects in intermolecular interactions. It has been shown that nonelectrostatic effects such as charge transfer between donor and acceptor are important in H-bonding and that for certain systems such as methyl-substituted amines continuum models lead to erroneous results.[58b] This deficiency is also present in discrete molecular mechanics models such as free energy perturbation because the atomic charges used in modern force fields are usually fitted to molecular *electrostatic* potentials. Thus, in addition to the continuum models used we employ a discrete solvent approach that entails a quantum mechanical description of the solute and the main features of the first solvation shell. A similar approach has been presented by several authors for aqueous solution.[60]

Hence, a supermolecule was constructed from solute molecules **1**−**3** and three surrounding DMSO molecules (Figure 7). This number of solvent molecules was considered to be essential to describe the H-bonding features of the solute, but still computationally tractable. Several initial supermolecular geometries were investigated for each tautomer, to map out the potential energy hypersurface for the solute:$(DMSO)_3$ complexes. Between 10 and 15 initial solute:$(DMSO)_3$ conformations were investigated for each of the N3-H, N7-H, and N9-H amino tautomers of adenine, 2-MeS-adenine and 8-Br-adenine. The initial conformations were generated either manually or by molecular dynamics annealing simulations. Each supermolecule was optimized to obtain a local minimum, and thus, a family of conformers was obtained for each tautomer (Figure 8). Thus, after B3LYP/6-31G(d,p) optimization, about 8−10 distinct conformers corresponding to local minima on the supermolecule energy hypersurface were obtained. The final energy of association for each tautomer with the three DMSO molecules describing the first solvation shell was obtained by summing the statistically weighed contribution of each conformer. For a full description of the approach, see the Methods.

The relative solvation energies for the N3-H, N7-H, and N9-H amino tautomers of adenine, 2-MeS-adenine, and 8-Br-adenine are presented in Table 4. Comparing the two continuum models, PB and PCM, quantitative agreement is observed in all cases. Solvation of the N7-H-tautomer of adenine, 2-MeS-adenine, and 8-Br-adenine is about 5 kcal/mol more favorable than that of the N9-H tautomers. Furthermore, the corresponding N3-H tautomers are also better solvated than the N9-H tautomer with relative energies ranging from −2.1 kcal/mol to −5.9 kcal/mol. The lower polarity of the three N9-H tautomers, as reflected in the lower molecular dipole moments (Table 3), is probably the reason for the lower relative solvation energies.

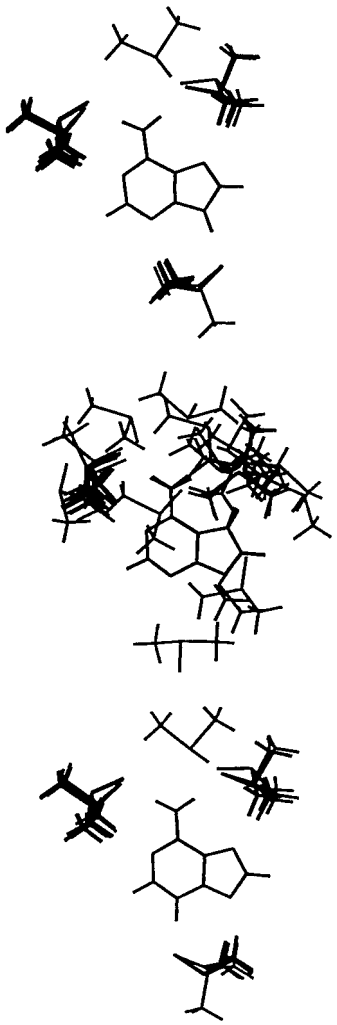

Figure 8. Distribution of DMSO solvent molecules around the N9-H (top), N7-H (middle), and N3-H (bottom) tautomers of adenine.

The explicit solvent model agrees qualitatively with the continuum models (Table 4). The relative solvation energy of N7-H-adenine is similar to that obtained with the continuum models. The relative solvation energy of N3-H-adenine is slightly greater than that obtained using the continuum models. In the case of the 8-Br- and the 2-MeS-adenine derivatives the explicit model gave results similar to that of the continuum models, although the differences in solvation energy between the N9-H tautomers and the N7-H and N3-H tautomers were somewhat larger.

The structures of the most stable complexes for each tautomer of adenine, 2-MeS-adenine and 8-Br-adenine may provide an insight into the reasons for the different solvation energies at the molecular level (Figure 7). The most stable complexes for the N9-H and N3-H tautomers of adenine and its derivatives were the ones that maximize the number of interactions between the solute and solvent molecules. Analysis of the complexes of the N9-H and N3-H tautomers of adenine, 2-MeS-adenine and 8-Br-adenine reveals that the N3-H isomer has tighter H-bonds than the N9-H isomer (Figure 7). The three classical H-bonds between the DMSO oxygen and the N3-H-adenine N-H hydrogens are shorter than those of the

(59) (a) Tomasi, J.; Persico, M. Molecular interactions in solution: An overview of methods based on continuous distribution of the solvent. *Chem. Rev.* **1994**, *94*, 2027−2094. (b) Cramer, C. J.; Truhlar, D. G. Implicit solvation models: equilibria, structure, spectra, and dynamics. *Chem. Rev.* **1999**, *99*, 2161−2200. (c) Orozco, M.; Luque, F. J. Theoretical methods for the description of the solvent effect in biomolecular systems. *Chem. Rev.* **2000**, *100*, 4187−4225.

(60) (a) Montero, L. A.; Esteva, A. M.; Molina, J.; Zapardiel, A.; Hernández, L.; Márquez, H.; Acosta, A. A theoretical approach to analytical properties of 2,4-diamino-5-phenylthiazole in water solution. Tautomerism and dependence on pH. *J. Am. Chem. Soc.* **1998**, *120*, 12023−12033. (b) Calvo-Losada, S.; Suárez, D.; Sordo, T. L.; Quirante, J. J. Competition between Wolff rearrangement and 1,2-hydrogen shift in β-oxy-α-ketocarbenes: Electrostatic and specific solvent effects. *J. Phys. Chem. B* **1999**, *103*, 7145−7150. (c) Shukla, M. K.; Leszczynski, J. A DFT investigation on effects of hydration on the tautomeric equilibria of hypoxanthine. *THEOCHEM* **2000**, *529*, 99−112.

Table 4. Relative Free Energies of Solvation for Adenine (Ad), 2-MeS-adenine (2-MeS-Ad), and 8-Br-adenine (8-Br-Ad) Amino Tautomers in DMSO Solution

	$\Delta\Delta G^{solvation}$ (kcal/mol)			
	Poisson−Boltzmann[a]	PCM[b]	explicit solvent model[c]	dipole moment[d] (D)
Ad-9H	0	0	0	6.33
Ad-7H	−5.55	−5.64	−5.31	5.36
Ad-3H	−3.89	−3.39	−5.18	6.22
2-MeS-Ad-9H	0	0	0	7.47
2-MeS-Ad-7H	−5.58	−5.35	−7.67	7.45
2-MeS-Ad-3H	−2.61	−2.08	−4.01	7.28
8-Br-Ad-9H	0	0	0	6.69
8-Br-Ad-7*H*	−5.04	−5.34	−6.08	7.69
8-Br-Ad-3*H*	−5.52	−5.89	−6.65	5.85

[a] The free energy of solvation was calculated as the difference in energy between the optimized solute in solution phase and the gas phase at the B3LYP/6-31G(d,p) level. [b] The free energy of solvation was calculated as the difference in energy between the optimized solute in solution phase and the gas phase at the B3LYP/6-31G(d) level. [c] The solvation energy was approximated as the association energy of the solute with three DMSO solvent molecules making up the first solvation shell. Computed at the B3LYP/6-31++G(d,p)//B3LYP/6-31G(d,p) level. The LAV3P** basis set was used for the S and Br atoms. [d] Dipole moments of the most stable solute:$(DMSO)_3$ complexes.

N9-H tautomers by 0.01−0.05 Å in almost all cases. Moreover, the weak H-bonds between the methyl hydrogens of DMSO and the adenine ring nitrogens are also tightened in most cases for the N3-H tautomers (values not shown). Thus, it seems that the greater solvation energy of the N3-H tautomer relative to that of the N9-H tautomer is due to the formation of stronger H-bonds with the surrounding solvent molecules.

In the case of the N7-H tautomer of compounds **1**−**3**, the most stable complex is the one that maximizes the number of solute−solvent and solvent−solvent interactions (Figure 9). A tight network of solute−solvent and solvent−solvent strong and weak H-bonds is formed. In this conformation, the supermolecule avoids being overcrowded, which is the case when all three DMSO molecules are directed toward the adenine N^6 and N7 hydrogens, while maximizing the total number of interactions. This network of H-bonds in the N7-H supermolecule results in a solvation energy that is greater than that of the N9-H isomer and greater or equal to that of the N3-H tautomer.

How well does such an explicit solvent approach represent actual solvation? The solvation energy is usually divided into three contributions: cavitation, dispersion−repulsion, and electrostatics. In our discrete solvent description, the cavitation energy is ignored. However, the cavitation energy for molecules of similar size, such as tautomers of a certain species, is expected to be similar. Moreover, long-range electrostatic interactions (i.e., solute−bulk solvent interactions) are not accounted for. An estimation of such long-range electrostatic interactions may be achieved by inspecting the supermolecular dipole moments (Table 4). The dipole moments of the most stable complexes of the three DMSO molecules with the N9-H, N7-H, and N3-H tautomers of adenine were 6.3, 5.4, and 6.2 D, respectively. In the case of the three thiomethyl-adenine tautomers the supermolecule dipole moments were almost identical, with values between 7.3 and 7.5 D. For the bromine adenine tautomers, the dipole moments ranged between 5.9 and 7.7 D. Thus, assuming

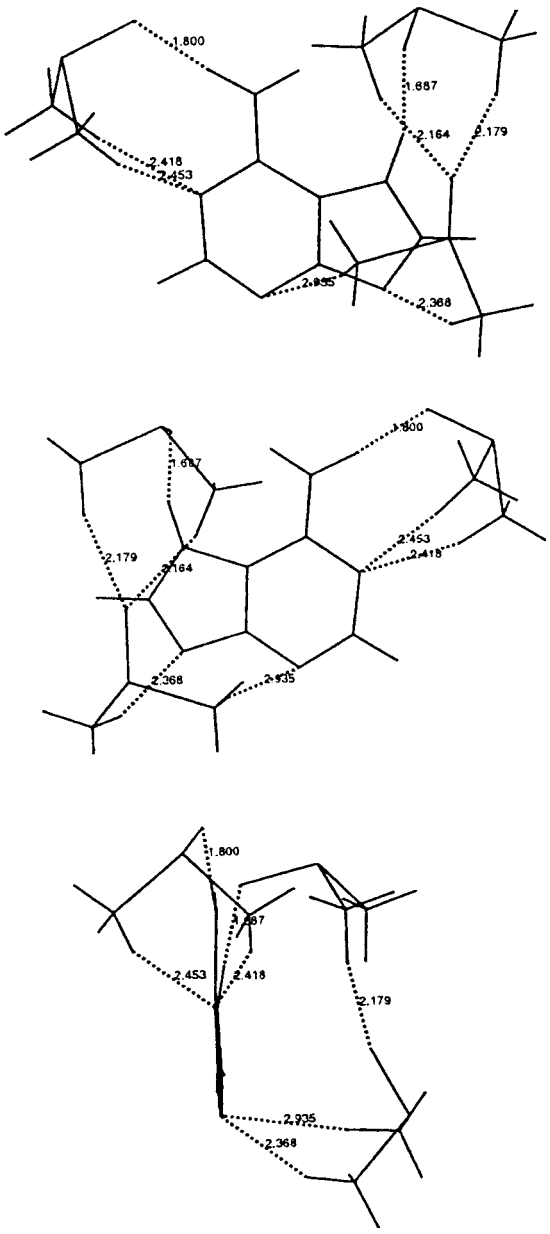

Figure 9. Network of H-bonds in the N7-H tautomer of adenine.

that any additional solvation may be treated by a continuum model, it may turn out that such effects would be similar for the three tautomers. In summary, this explicit solvent approach is expected to produce reliable estimations of the solvation energy, while providing a detailed description of the solute−solvent interactions.

However, caution should be exercised when drawing conclusions regarding the explicit solvation model. There is no guarantee that the global minimum supermolecular conformation was found. Moreover, the effect of additional first solvation shell molecules and the added effect of bulk solvation, including solvent reorganization, were not investigated explicitly.

In light of the agreement in the relative energies of solvation between the continuum and explicit solvation models, the solution-phase tautomerization could be analyzed using any of the solvation model results. However, the solvation energy is not well defined within the discrete solvent approach as it is in continuum models.

Table 5. Relative Free Energies[a] of Adenine (Ad), 2-MeS-adenine (2-MeS-Ad), and 8-Br-adenine (8-Br-Ad) Amino Tautomers in DMSO Solution

	$\Delta G^{tautomer}$ (kcal/mol)		
	9H	7H	3H
Ad	0	2.24	3.47
2-MeS-Ad	0	1.87	6.15
8-Br-Ad	0.42	3.03	0

[a] The gas-phase part of the free energy was calculated using B3LYP/Aug-cc-pVTZ//B3LYP/6-31G(d). The free energy of solvation was calculated using the SCRF-PB model.

Therefore, in the coming discussion of the calculations and comparisons with NMR results we refer to the solvation free energy obtained from the PB model.

The tautomeric energies of N3-H and N7-H relative to that of N9-H are significantly reduced in a DMSO solution. The reason for this is the greater polarity of the N3-H and N7-H tautomers relative to N9-H (Table 3), which leads to a greater free energy of solvation. Still, in the case of adenine and 2-MeS-adenine the equilibrium is in favor of the N9-H-amino tautomer (Table 5). However, the energy difference between the N9-H and N7-H isomers is now only about 2 kcal/mol. Interestingly, N3-H-adenine is only slightly less stable than N7-H-adenine—the difference between them being 1.2 kcal/mol (Table 5). Thus, we predict that the N3-H tautomer of adenine exists in solution in addition to the N9-H and N7-H isomers, as is seen in its ^{15}N NMR spectrum (Figure 2A). However, 2-MeS-N3-H-adenine is considerably less stable than the N9-H and N7-H isomers, probably due to steric hindrance between the thioether group and the N3-H. 2-MeS-adenine-N3-H is less stable than the corresponding N7-H tautomer by ca. 4 kcal/mol. This is in agreement with experimental results (Figure 4).

The calculations for 8-Br-adenine, **3**, predict reversal of the relative stability of the tautomers (Table 5). In 8-Br-adenine, the N3-H tautomer is predicted to be slightly more stable than the N9-H tautomer, the difference between them being 0.4 kcal/mol, while the N7-H isomer was found to be 3.0 kcal/mol less stable (Table 5).

Conclusions

The assembly of five ^{15}N atoms to form adenine in four synthetic steps, in a reasonable yield, is reported here. Likewise, ($^{15}N_5$)-2-hexylthioether-adenine and ($^{15}N_5$)-8-Br-adenine were obtained in five synthetic steps from the relatively inexpensive ^{15}N sources: ^{15}N-NH_4Cl, ^{15}N-NH_4-OH, ^{15}N-$NaNO_2$. Full ^{15}N labeling of these adenine prototypes, **1**−**3**, enabled to obtain high-resolution ^{15}N NMR spectra of these bases. Furthermore, these spectra suggested the existence of the N3-H tautomer in the tautomeric mixtures of compounds **1** and **3** in solution, in addition to the well-reported N9-H major tautomer, and N7-H minor tautomer. These observations were also supported by quantum mechanical calculations of the tautomeric equilibria of these prototype adenine compounds, in solution. Both the gas-phase and solution-phase calculations were performed using inherently different computational methods to add confidence to the results. In the gas phase, second-order perturbation theory and density functional theory calculations were performed, while solvent effects were included using both a continuum and discrete description of solvation. The observation of the existence of the N3-H tautomer in solution has a clear impact on the possible H-bonding patterns of these adenine prototypes, and on their molecular recognition by various biological macromolecules.^{15}N labeled analogues **1-3** are expected to find use as ^{15}N NMR probes for numerous biochemical studies. The use of these analogues for the synthesis of ($^{15}N_5$)-adenine nucleosides, their properties, and their interaction with proteins will be reported in due course.

Experimental Section

General Methods. NMR spectra were recorded on a Bruker DPX-300 instrument (300.1, 75.5, and 30.4 MHz for ^1H, ^{13}C, and ^{15}N, respectively) or on a Bruker DMX-600 instrument (600.1, 150.9, and 60.8 MHz for ^1H, ^{13}C, and ^{15}N, respectively). ^{15}N NMR spectra were recorded with nitromethane ($\delta = 0$ ppm) as an external standard at 0.07−0.2 M concentration range. Negative chemical shifts are upfield from nitromethane. Difficulties in obtaining ^{15}N spectra with good signal-to-noise ratios are quite common due to the negative nuclear Overhauser effect that results from the negative magnetogyric ratio of the ^{15}N nucleus and also the relative long T_1 relaxation times. To obtain the necessary data, spectra were recorded in more than one of the following techniques: with proton coupling, proton decoupling, and inverse gated. Products were also characterized on an AutoSpec-E fision VG high-resolution mass spectrometer. The purity of the new compounds was evaluated on HPLC (Merck-Hitachi) using an analytical column (LiChroCART LiChrospher 60RP-select B column (250 mm × 4.6 mm), Merck KGaA) using two different solvent systems. Solvent system I: MeOH/H_2O, 50:50−90:10 in 25 min. Solvent system II: CH_3CN/H_2O, 50:50. Flow rate was 1 mL/min. $^{15}NH_4Cl$ (99% atom ^{15}N) and ^{15}N-$NaNO_2$ (min 99% atom ^{15}N) were purchased from Isotec Inc., USA. ($^{15}N_2$)-Thiourea (96% atom ^{15}N) and $^{15}NH_4$-OH (98% atom ^{15}N) were purchased from Euriso-top, France, and from Cambridge Isotope Laboratories Inc., USA, respectively. The preparation of nonlabeled adenine, 2-thioether-adenine, and 8-Br-adenine, via synthetic routes different than those described below, was reported previously.[33b,25a,61]

($^{15}N_5$)-Adenine (1). Compound **1** was obtained by desulfurization of **2**. 2-Hexylthioether-adenine **2** (57 mg, 0.22 mmol) was dissolved in 1 N NaOH solution (8 mL) with slight heating. Ra-Ni (1 mL, of 50% water suspension) was added to the clear solution, over 5 min, and this mixture was refluxed for 2 h. The Ra-Ni was separated from the reaction mixture by centrifugation, and the resulting basic solution was neutralized with concentrated HCl solution. The solvent was evaporated, and the resulting white residue was purified by column chromatography on silica gel ($CHCl_3$/MeOH 70:30). The product was obtained as a white solid in 25% yield (8 mg). ^1H NMR (DMSO-d_6, 600 MHz) δ: 8.12 (t, $^2J_{NH} = 15.5$ Hz, H-2), 8.03 (ddd, $^2J_{NH} = 11.5$, 10 Hz, $J = 0.6$ Hz, H-8), 6.67 (d, $^1J_{NH} = 89.5$ Hz, NH_2). ^{13}C NMR (DMSO-d_6, 75.5 MHz) d: 155.1 (C-6), 152.4 (C-2), 151.2 (C-4), 139.3 (C-8), 118.3 (C-5). ^{15}N NMR (DMSO-d_6, 61 MHz) δ: −140.3 (N-7), −145.7 (ddt, $^2J_{NH} = 15.5$ Hz, $^2J_{NN} = 5.5$ Hz, $^3J_{NH} = 4$ Hz, N-1), −151.5 (N-3), −222.6 (N-9), −301.2 (td, $^1J_{NH} = 89.5$ Hz, $^2J_{NH} = 5.5$ Hz, NH_2). HRMS (DCI, CH_4): calcd for $C_5H_615N_5$ (MH^+) 141.0474, found 141.0470.

($^{15}N_5$)-2-Hexylthioether-adenine (2). A mixture of **12** (63 mg, 0.25 mmol), trimethyl orthoformate (4 mL), and concentrated hydrochloric acid (0.5 mL) was stirred at room temperature for 15 min. The resulting solution was evaporated, and the residue was chromatographed on a silica gel column ($CHCl_3$/MeOH, 95:5). The product was obtained as an oily residue in 85% yield (54.4 mg). Alternatively, **2** could obtained by the following procedure: a solution of **12** (256 mg, 1.04

(61) Beaman, A. G.; Gerster, J. F.; Robins, R. K. Potential purine antagonists. XXVII. Preparation of bromopurines. *J. Org. Chem.* **1962**, *27*, 986−990.

mmol) in formamide (5 mL) was heated under reflux for 1 h. After the mixture was cooled to room temperature, water (5 mL) was added. The product, which precipitated from the solution as a yellow-brownish solid, was filtered and washed with cold water. The product was purified on a silica gel column (elution with EtOAc/Et_2O 1:1) and collected as a pale yellow solid in 80% yield (214 mg). ^{1}H NMR (CD_3OD, 600 MHz) δ: 7.95 (t, $^2J_{NH}$ = 9.5 Hz, H-8), 3.14 (t, J = 7.3 Hz, 2H, SCH_2), 1.46 (quintet, J = 7.5 Hz, 2H, SCH_2CH_2), 1.46 (m, 2H), 1.37−1.30 (m, 4H), 0.90 (t, J = 7 Hz, 3H, CH_3). ^{13}C NMR (CD_3OD, 75.5 MHz) δ: 166.6 (C-2), 155.9 (C-6), 150.3 (C-4), 139.8 (d, $^1J_{NC}$ = 15 Hz, C-8), 116.0 (C-5), 32.5 (SCH_2CH_2), 31.7 (t, $^3J_{NC}$ = 2.9 Hz, SCH_2), 30.6, 29.6, 23.5, 14.3 (CH_3). ^{15}N NMR (CD_3OD, 61 MHz) δ: −152.0 (N-7, broad), −157.3 (N-1, $^2J_{NN}$ = 6 Hz), −165.7 (N-3), −226.0 (N-9, broad), −308.1 (NH_2, $^2J_{N-N}$ = 6 Hz, $^1J_{NH}$ = 91 Hz). HRMS (DCI, CH_4): calcd for $C_{11}H_{18}{}^{15}N_5S$ (MH^+) 257.1134, found 257.1138.

($^{15}N_5$)-8-Bromo-adenine (3). A solution of bromine (0.1 mL, 1.96 mmol) in water (15 mL) was added to adenine **1** (140 mg, 1 mmol). After being stirred at room temperature overnight, in a stoppered flask, the reaction mixture was evaporated under high vacuum. The yellow residue was separated on a silica gel column ($CHCl_3$/MeOH 9:1). The product was obtained as a yellow solid in 83% yield (181 mg). ^{1}H NMR (DMSO-d_6, 300 MHz) δ: 8.13 (t, $^2J_{NH}$ = 14.4 Hz, H-2), 5.46 (d, $^1J_{NH}$ = 88 Hz, NH_2). ^{15}N NMR (DMSO-d_6, 61 MHz, 350K) δ: −139.7 (N-7), −144.8 (N-1), −151.5 (N-3), −224.2 (N-9), −305.1 (NH_2, $^1J_{NH}$ = 88.2 Hz). HRMS: calcd for $C_5H_4{}^{15}N_5Br$ (MH^+) 217.9501, 219.9481, found 217.9527, 219.9501.

($^{15}N_2$)-Thiourea (5). ($^{15}N_2$)-Ammonium thiocyanate was prepared according to literature procedure[29a] for 2.0 g (36.6 mmol) of $^{15}NH_4Cl$. However, isolation of the product was completely modified. At the end of the reaction, the solution's pH was corrected to 5.5 with concentrated HCl solution. The mixture was filtered, and the precipitate was washed with ice-cold EtOH. The filtrate was evaporated and washed with MeOH and acetone. The solvents were evaporated, and the residue was separated on a silica gel column (elution started from 10% MeOH in $CHCl_3$ to 50%). The product was contaminated by NaSCN. An aqueous solution of this mixture was passed through a cation exchanger column (Chelex-100, Bio-Rad) loaded with $^{15}NH_4Cl$. The solution was freeze-dried to give the desired product in 95% yield (1.37 g). ^{13}C NMR (D_2O, 75.5 MHz) δ: 133.7 (d, $^1J_{CN}$ = 14 Hz). ^{15}N NMR (acetone-d_6, 30 MHz) δ: −183.9 (SCN^-), −306.3 (t, $^1J_{NH}$ = 91 Hz, $^+NH_4$). ($^{15}N_2$)-Thiourea was obtained upon heating ($^{15}N_2$)-NH_4SCN in a sealed tube at 190 °C for 2 h. The residue consisting a mixture of ($^{15}N_2$)-NH_4SCN and ($^{15}N_2$)-thiourea, in a 1:6 ratio (respectively), was separated on a silica gel column. The elution started from 20% $CHCl_3$ in EtOAc to 100% EtOAc. To obtain the NH_4SCN, MeOH is added gradiently, starting from 10% to 50% MeOH in EtOAc. NH_4SCN and thiourea could be visualized on TLC (in EtOAc) by staining with $KMnO_4$ solution. The TLC plate turns purple and the above compounds are seen as a yellow stain, NH_4SCN with R_f 0.25 and thiourea with R_f 0.37. ^{13}C NMR (acetone-d_6, 151 MHz) δ: 185.7 (t, $^1J_{C-N}$ = 15.7 Hz). ^{15}N NMR (acetone-d_6, 30 MHz) δ: 277.6 (t, $^1J_{NH}$ = 91 Hz). HRMS (DCI, CH_4): calcd for $CH_5{}^{15}N_2S$ (MH^+) 79.0114, found 79.0092.

($^{15}N_4$)-4,6-Diamino-2-mercaptopyrimidine (6) was prepared according to literature procedure.[28b,c] ^{13}C NMR (DMSO-d_6 + NaOH, 75.5 MHz) δ: 184.3 (C-2), 162.5 (d, $^1J_{C-N}$ = 18 Hz, C-4, C-6), 76.7 (C-5). ^{15}N NMR (DMSO-d_6, 30 MHz) δ: −155.9 (N-1, N-3), −308.6 (t, $^1J_{NH}$ = 90 Hz, NH_2). HRMS (DCI, CH_4): calcd for $C_4H_7{}^{15}N_4S$ (MH^+) 147.0272, found 147.0270.

($^{15}N_5$)-4,6-Diamino-2-mercapto-5-nitrosopyrimidine (7) was prepared according to literature procedure.[28b,c] ^{13}C NMR (DMF-d_7, 75.5 MHz) δ: 175.2 (t, $^1J_{CN}$ = 4 Hz, C-2), 165.9 (ddd, $^1J_{CN}$ = 22 Hz, $^2J_{CN}$ = 7, 4 Hz, C-5), 146.4 (dd, $^1J_{CN}$ = 18.8 Hz, $^1J_{CN}$ = 2 Hz, C-4 or C-6), 139.7 (d, $^1J_{CN}$ = 9.8 Hz, C-4 or C-6). ^{15}N NMR (DMF-d_7, 30 MHz) δ: 343.3 (t, $^3J_{NN}$ = 1.5 Hz, NO), −165.5 (2nd order triplet, N-1, N-3), −292.8 (td, $^1J_{NH}$ = 91 Hz, $^2J_{NN}$ = 5.5 Hz, NH_2), −294.1 (td, $^1J_{NH}$ = 92.5 Hz, $^2J_{NN}$ = 5.5 Hz, NH_2). HRMS (DCI, CH_4): calcd for $C_4H_6{}^{15}N_5OS$ (MH^+) 177.0144, found 177.0158.

($^{15}N_5$)-4,5,6-Triaminopyrimidine (8). To a solution of **7** (80 mg, 0.45 mmol) in DMF (5 mL) was added Raney nickel (1 mL of 50% water suspension) over 5 min. After being stirred at room temperature overnight, the reaction mixture was filtered through a bed of Celite, and the Raney nickel filter cake was washed with DMF. The filtrate was concentrated to give a brownish oil in 43% yield (25 mg). ^{13}C NMR (DMF-d_7, 75.5 MHz) δ: 152.7 (d, $^1J_{CN}$ = 18 Hz, C-4, C-6), 148.4 (C-H), 107.3 (C-5). ^{15}N NMR (DMF-d_7, 61 MHz) δ: −145.9 (N-1, N-3), −313.7 (t, $^1J_{NH}$ = 86.4 Hz, 4,6-NH_2), −349.8 (5-NH_2). HRMS (DCI, CH_4): calcd for $C_4H_8{}^{15}N_5$ (MH^+) 131.0631, found 131.0697.

($^{15}N_4$)-4,6-Diamino-2-hexylthiopyrimidine (10). A suspension of **6** (220 mg, 1.51 mmol, in 20 mL MeOH) was dissolved in 0.25 M NaOH (6.35 mL) and stirred at room temperature for 1 h. The solvent was evaporated under high vacuum. The dry sodium thiolate salt was dissolved in dry DMF (20 mL), and bromohexane (0.21 mL, 1.51 mmol) was added. The clear brown solution was stirred at room temperature overnight. TLC ($CHCl_3$/MeOH 9:1) indicated that all starting material was consumed. The solvent was evaporated under high vacuum, and the brown residue was separated on a silica gel column ($CHCl_3$/MeOH 95:5). The product was obtained as a yellow oil in 89% yield (309 mg). t_R: 15.98 min (97.7% purity) using solvent system I, 7.78 min (99.9% purity) using solvent system II. ^{1}H NMR (CD_3OD, 300 MHz) δ: 3.07 (t, J = 7.2 Hz, 2H, SCH_2), 1.69 (quintet, J = 7.2 Hz, 2H, SCH_2CH_2), 1.52−1.29 (m, 6H), 0.94 (t, J = 6.5 Hz, 3H, CH_3). ^{13}C NMR (CD_3OD, 75.5 MHz) δ: 170.5 (tt, $^1J_{CN}$ = 3 Hz, $^3J_{CN}$ = 1.5 Hz, C-2), 164.5 (dm, $^1J_{CN}$ = 19 Hz, C-4,C-6), 80.1 (tt, $^2J_{CN}$ = 4.5, 1.5 Hz, C-5), 32.1 (SCH_2CH_2), 30.7 (t, $^3J_{CN}$ = 2.9 Hz, SCH_2), 30.2, 29.1, 23.1, 13.9 (CH_3). ^{15}N NMR (CD_3OD, 30 MHz) δ: −166.3 (d, $^2J_{NN}$ = 5.5 Hz, N1,N3), −309.1 (td, $^2J_{NN}$ = 5.5 Hz, $^1J_{NH}$ = 88 Hz, 4,6-NH_2). HRMS (DCI, CH_4): calcd for $C_{10}H_{18}{}^{15}N_4S$ (M^+) 230.1133, found 230.1138.

($^{15}N_5$)-4,6-Diamino-5-nitroso-2-hexylthiopyrimidine (11). To a chilled solution, at 0 °C, of **10** (300 mg, 1.3 mmol) in acetic acid (6 mL) and water (1.2 mL) was added (^{15}N)-sodium nitrite (164 mg, 2.34 mmol) in water (1.2 mL) during 15 min. The resulting pink suspension was stirred at 0 °C for 15 min, and the product was isolated by suction filtration and washed with cold water. The gray-blue filter cake was dried to give **11** in 75% yield (253 mg). Mp: 110−112 °C. t_R: 19.27 min (97.7% purity) using solvent system I, 7.98 min (97.8% purity) using solvent system II. ^{1}H NMR (CD_3OD, 300 MHz) δ: 3.17 (t, J = 7.2 Hz, 2H, SCH_2), 1.73 (quintet, J = 7.5 Hz, 2H, (SCH_2CH_2), 1.53−1.31 (m, 6H), 0.94 (t, J = 6.9 Hz, 3H, CH_3). ^{13}C NMR (CD_3OD, 151 MHz) δ: 182.0 (t, $^1J_{CN}$ = 3.6 Hz, C-2), 166.0 (ddd, $^1J_{CN}$ = 22.2 Hz, $^2J_{CN}$ = 7.5 Hz, $^2J_{CN}$ = 4.8 Hz, C-5), 148.0 (dd, $^1J_{CN}$ = 19.7 Hz, $^2J_{CN}$ = 3.2 Hz, C-4 or C-6), 139.7 (d, $^1J_{CN}$ = 8 Hz, C-4 or C-6), 32.6, 32.0 (t, $^3J_{CN}$ = 3.1 Hz, SCH_2), 30.7, 30.6, 29.6, 23.6, 14.3 (CH_3). ^{15}N NMR (CD_3OD, 61 MHz) δ: 308.2 (NO), −168.0 (d, $^2J_{NN}$ = 5.5 Hz, N-1 or N-3), −168.3 (d, $^2J_{NN}$ = 4.2 Hz, N-1 or N-3), −293.2 (t, $^1J_{NH}$ = 91.8 Hz, NH_2), −298.9 (t, $^1J_{NH}$ = 88.2 Hz, NH_2). HRMS (DCI, CH_4): calcd for $C_{10}H_{18}{}^{15}N_5OS$ (MH^+) 261.1083, found 261.1115.

($^{15}N_5$)-4,5,6-Triamino-2-hexylthiopyrimidine (12). Compound **11** (30 mg, 0.11 mmol) dissolved in EtOH (2 mL) was hydrogenated at atmospheric pressure, for 3 h, at room temperature, over PtO_2 catalyst. The reaction mixture was filtered through a bed of Celite. The filtrate was concentrated and dried to give **12**, as an oily solid, in a quantitative yield. t_R: 14.90 min (98.2% purity) using solvent system I, 5.52 min (99.7% purity) using solvent system II. ^{1}H NMR (CD_3OD, 300 MHz) δ: 3.04 (t, J = 7.2 Hz, 2H, SCH_2), 1.67 (quintet, J = 6.9 Hz, 2H, SCH_2CH_2), 1.48−1.28 (m, 6H), 0.92 (t, J = 6.5 Hz, CH_3). ^{13}C NMR (CD_3OD, 75.5 MHz) δ: 162.0 (C-2), 156.6 (dd, $^1J_{CN}$ = 18 Hz, $^1J_{CN}$ = 4 Hz, C-4, C-6), 102.4 (d, $^1J_{CN}$ = 10 Hz, C-5), 32.6 (SCH_2CH_2), 31.6 (t, $^3J_{CN}$ = 3 Hz, SCH_2), 30.8, 29.6, 23.6, 14.4 (CH_3). ^{15}N NMR (CD_3OD, 61 MHz) δ: −162.1 (d, $^2J_{NN}$ = 5 Hz, N-1, N-3), −314.6 ($^1J_{NH}$ = 87 Hz, $^2J_{NN}$ = 5 Hz, 4,6-NH_2), −359.3 (5-NH_2). HRMS (DCI, CH_4): calcd for $C_{10}H_{19}{}^{15}N_5S$ (M^+) 246.1212, found 246.1200.

Computational Methods

The free energy of tautomerization was calculated according to:

$$\Delta G^{aq}(A \rightarrow B) = \Delta G^{gas}(A \rightarrow B) + \Delta G^{solv}(B) - \Delta G^{solv}(A) = \Delta G^{gas}(A \rightarrow B) + \Delta\Delta G^{solv}(A \rightarrow B) \quad (1)$$

The twelve amino tautomers of 2-MeS-adenine and 8-Br-adenine were optimized using the B3LYP functional[52] with the 6-31G(d) basis set.[54] For adenine, only the N3-H, N7-H, and N9-H-amino tautomers were optimized on the basis of previous reports.[50] Vibrational frequencies were calculated to examine the nature of the stationary points on the potential energy surface. No negative frequencies were found. All optimized structures were nonplanar. Single-point gas-phase calculations were calculated for the N3-H, N7-H, and N9-H-amino tautomers of adenine, 2-MeS-adenine, and 8-Br-adenine using the B3LYP and MP2[53] methods with the 6-311+G(2df,2p) basis set.[55] This is a triple split valence basis supplemented by diffuse functions, two sets of d- and one set of f-type polarization functions on heavy atoms and two sets of p-type polarization functions on hydrogens. B3LYP single point calculations were also calculated using the cc-pVTZ basis set[56] augmented with diffuse functions. The MP2 calculations were performed with the frozen core approximation. To these energies, B3LYP/6-31G(d) thermal corrections at a temperature of 298.15 K were added using scaling factors of 0.9806, 0.9989, and 1.0015 for the zero-point energy, enthalpy, and entropy, respectively.[62]

Free energies of solvation were calculated using the polarizable continuum model (PCM)[57] and the SCRF Poisson−Boltzmann (SCRF−PB)[58] method. In both PCM and SCRF-PB the solute is embedded in a van der Waals surface-type cavity surrounded by a polarizable medium with the dielectric constant of the solvent. In PCM, which solves the Laplace equation, the computed solute electrostatic potential is used to determine the solvent reaction field, i.e., the polarization of the solvent. In SCRF-PB, which solves the Poisson equation, atomic charges fitted to the electrostatic potential are used to represent the solute charge distribution, which induces a reaction field in the continuum solvent. In both approaches, the solute charge distribution is allowed to relax in the presence of the reaction field until self-consistency is achieved. The solvation energy was calculated as the difference between the energy of the optimized solvated structure and the optimized gas-phase structure. In PCM B3LYP/6-31G(d) was used and in SCRF-PB the B3LYP/6-31G(d,p) functional was used. All calculations were performed using DMSO as the solvent ($\epsilon = 46.7$). The PCM calculations were performed with the Pauling atomic radii and default scaling factors. In addition, the following keywords were used: tsare = 0.4, icomp = 2 (geometry optimization), icomp = 4 (single-point calculations). For the 2-MeS-adenine-9H tautomer the calculation failed with tsare = 0.4; using tsnum = 100 the calculation succeeded. In SCRF-PB the probe radius was set to 2.352. In both the PCM and PB calculations only the electrostatic contribution to the solvation energy was included.

The solvation energy was also estimated by a discrete model, which embedded the solute within an approximate first solvation shell constituting three DMSO molecules. The initial structures were generated either manually or by molecular dynamics annealing simulations. The manually created structures were built to maximize the number of solute−solvent and solvent−solvent interactions. This was done by graphical manipulation of the structures using the Maestro program (Schrödinger, Inc. Pasadena, CA, 2000). The molecular dynamics simulations were performed by placing the solute in a 35 Å thick spherical shell of DMSO molecules. The outer 10 Å of this shell was constrained to avoid the escape of solvent molecules. Initially, to remove bad steric interactions, the system was minimized for 300 iterations using the steepest descent method, followed by 300 iterations of the Polak-Ribiere conjugate gradient method. Then the system was heated to 1000 °K and equilibrated for 5000 fs. Thereafter, the system was cooled to 300 °K in six steps of 400 fs each. This annealing process was expected to lead to low energy configurations of the solute−solvent system. After the cooling process the system was minimized again to remove bad contacts. The last step was a 5000 fs simulation, which generated configurations of the solute−solvent system. The time step in all the simulations was 1 fs. The simulations were performed using the Amber95 force field[63] and parameters of Kollmann et al. for DMSO[64] were added. The solute and the three nearest DMSO molecules were extracted from the solute−solvent system and used as initial structures for the next step.

The generation step led to about 10−15 initial structures of N1-H, N3-H, and N9-H amino tautomers of adenine, 2-MeS-adenine, and 8-Br-adenine complexed with three DMSO solvent molecules. These structures were optimized using the B3LYP functional in a stepwise manner. Initially, the solute−solvent systems were optimized using the 6-31G basis set and polarization functions were added for the atoms involved in classical H-bonding (DMSO oxygen and adenine ring N-H). These initial optimizations were performed with loose SCF and optimization convergence criteria (econv = 5E−4, dconv = 5E−5, and iaccg = 3 keywords in Jaguar 4.0), and the H-bond distances were constrained to about 1.8 Å. In the subsequent optimization, all constraints were removed, and the basis set changed to 6-31G(d,p). Default optimization convergence criteria were used together with ultrafine grids and tight cutoffs (iacc = 1) in the SCF procedure and ultrafine DFT grids (gdftmed = −13, gdftfine = −13, gdftgrad = −13). The optimization process was followed by single point calculations at the B3LYP/6-31++G(d,p) level with ultrafine grids. In all cases, the LAV3P effective core potential basis set[65] was used for S and Br instead of the 6-31G basis set. All optimizations were performed in Cartesian coordinates. After the optimizations, about 8−9 distinct supermolecular conformers remained for each of the three amino isomers of adenine, 2-MeS-adenine and 8-Br-adenine. The energy of association of the *i*th complex was calculated as

$$\Delta E_i^{assoc} = E_i(S{\cdot}DMSO_3) - E(S) - 3{\cdot}E(DMSO) \quad (2)$$

where S is the solute. The statistical weight of each conformer was calculated by estimating their contribution to the total population assuming a Boltzmann distribution

$$p_i = \frac{e^{-\Delta E_i^{assoc}/RT}}{\sum_{i=1}^{n} e^{-\Delta E_i^{assoc}/RT}} \quad (3)$$

were p_i is the statistical weight of conformer i, the denominator is the approximate molecular partition function, and n is the number of conformers.

The solvation energy of each tautomer was estimated as the statistically weighed association energy of the complex

(62) Scott, A. P.; Radom, L. Harmonic vibrational frequencies: An evaluation of Hartree−Fock, Møller−Plesset, quadratic configuration interaction, density functional theory, and semiempirical scale factors. *J. Phys. Chem.* **1996**, *100*, 16502−16513.

(63) Cornell, W. D.; Cieplak, P.; Bayly, C. I.; Gould, I. R.; Merz, K. M. Jr.; Ferguson, D. M.; Spellmeyer, D. C.; Fox, T.; Caldwell, J. W.; Kollman, P. A. A second generation force field for the simulation of proteins, nucleic acids, and organic molecules. *J. Am. Chem. Soc.* **1995**, *17*, 5179−5197.

(64) Fox, T.; Kollman, P. A. Application of the RESP methodology in the parametrization of organic solvents. *J. Phys. Chem. B.* **1998**, *102*, 8070−8079.

(65) (a) Hay, P. J.; Wadt, W. R. Ab initio effective core potentials for molecular calculations. Potentials for the transition metal atoms Sc to Hg. *J. Chem. Phys.* **1985**, *82*, 270−283. (b) Wadt, W. R.; Hay, P. J. Ab initio effective core potentials for molecular calculations. Potentials for main group elements Na to Bi. *J. Chem. Phys.* **1985**, *82*, 284−298.

$$\Delta E^{\text{assoc}} = \sum_{i=1}^{n} p_i \cdot \Delta E_i^{\text{assoc}} \quad (4)$$

The basis set superposition error (BSSE) was estimated by the counter-poise correction[66] for the statistically most significant supermolecules ($p_i > 0.10$). This counter-poise correction was subtracted from the ΔE^{assoc} (eq 2) to obtain the corrected association energy for the complexes. A recent finding revealed that the BSSE is significant even for DFT models such as B3LYP and that it is as large as for MP2.[67]

The importance of the free rotation around the C2−S bond in 2-MeS-adenine in the gas phase was estimated by scanning the potential energy surface. The conformations were generated by rotating the C2−S bond by 30 degrees at each iteration, and performing single-point B3LYP/6-31G(d) calculations. Thus, an approximate population analysis was performed by assuming a Boltzmann distribution among all the possible conformations. The weighed average energy was found to be only about 0.3 kcal/mol above the lowest conformer, for all three most stable tautomers of 2-MeS-adenine in the gas phase and in solution.

The Gaussian 98 program[68] was used for all gas-phase calculations and PCM calculations. The SCRF-PB calculations and all calculations on the complexes employed the Jaguar 4.0 program.[69] The molecular dynamics simulations were performed using the Insight98/Discover package.[70] The calculations were performed on two SGI Origin 2000 (32xR12000) and several IBM Power PC machines.

Acknowledgment. The authors wish to thank the Marcus Centre for Medicinal Chemistry for financial support. D.T.M. thanks the Israeli Ministry of Science for financial support. We thank the reviewers and Editor for helpful suggestions.

JO010344N

(66) van Duijneveldt, F. B.; van Duijneveldt-van de Rijdt, J. G. C. M.; van Lenthe, J. H. State of the art in counterpoise theory. *Chem. Rev.* **1994**, *94*, 1873−1885.

(67) Rappé, A. K.; Bernstein, E. R. Ab initio calculation of nonbonded interactions: Are we there yet? *J. Phys. Chem. A.* **2000**, *104*, 6117−6128

(68) Frisch, M. J.; Trucks, G. W.; Schlegel, H. B.; Scuseria, G. E.; Robb, M. A.; Cheeseman, J. R.; Zakrzewski, V. G.; Montgomery, J. A.; Stratmann, R. E.; Burant, J. C.; Dapprich, S.; Millam, J. M.; Daniels, A. D.; Kudin, K. N.; Strain, M. C.; Farkas, O.; Tomasi, J.; Barone, V.; Cossi, M.; Cammi, R.; Mennucci, B.; Pomelli, C.; Adamo, C.; Clifford, S.; Ochterski, J.; Petersson, G. A.; Ayala, P. Y.; Cui, Q.; Morokuma, K.; Malick, D. K.; Rabuck, A. D.; Raghavachari, K.; Foresman, J. B.; Cioslowski, J.; Ortiz, J. V.; Stefanov, B. B.; Liu, G.; Liashenko, A.; Piskorz, P.; Komaromi, I.; Gomperts, R.; Martin, R. L.; Fox, D. J.; Keith, T.; Al-Laham, M. A.; Peng, C. Y.; Nanayakkara, A.; Gonzalez, C.; Challacombe, M.; Gill, P. M. W.; Johnson, B. G.; Chen, W.; Wong, M. W.; Andres, J. L.; Head-Gordon, M.; Replogle, E. S.; Pople, J. A. Gaussian 98 (Revision A.7), Gaussian, Inc., Pittsburgh, PA, 1998.

(69) Jaguar 4.0, Schrödinger, Inc., Pasadena, CA, 2000.

(70) Molecular Simulations Inc., San Diego, CA, 1998.